Paleoenvironmental constraints on Paleozoic shale deposition in the midcontinent United States

Noah Morris, Adriana Potra, and John R. Samuelsen

ABSTRACT

Trace element paleoenvironmental proxies were used to constrain depositional environments for several black shales of the midcontinent United States to better understand the formation of metalliferous shales. These shales range in age from Cambrian to Pennsylvanian. The proxies evaluated were for paleoredox (U/Th, U-[Th/3], Ni/Co, V/Cr, V/[V+Ni], Mo concentration, Mo/total organic carbon), basin restriction (Cd/Mo, Co × Mn) and paleosalinity (Sr/Ba). The results of the paleoredox proxies indicate a range of depositional conditions from oxic to dysoxic to anoxic. The findings suggest that the Cambrian Mt. Simon, Eau Claire, and Tunnel City samples in the northern part of the study area were deposited under oxic marine conditions influenced by upwelling. The Ordovician black shales from the Ouachita Mountains and the Pennsylvanian shales from the Cherokee and Forest City Basins were likely formed under anoxic, open marine conditions. The basin restriction and paleoredox proxies suggest decreasing oxygen levels during the deposition of the Ordovician shales, whereas the paleosalinity proxy, the Sr/Ba ratios, during this time suggests decreasing salinity. The Devonian Chattanooga Shale from the Ozark Dome and the New Albany Shale from the Illinois Basin were likely deposited under similar anoxic to dysoxic conditions. Paleoredox proxies suggest that the Mississippian Fayetteville Shale in the Ozark Dome formed under a range of oxic to anoxic conditions. Similarly, the Pennsylvanian Atoka and Jackfork Formations in the Ouachitas were deposited under oxic marine conditions. The results of this study also highlight the importance of using multiple proxies to interpret paleoenvironments.

Manuscript received December 5, 2022; provisional acceptance April 18, 2023; revised manuscript received June 26, 2023; revised manuscript provisional acceptance September 19, 2023; 2nd revised manuscript received October 10, 2023; 2nd revised manuscript provisional acceptance November 21, 2023; 3rd revised manuscript received December 6, 2023; 3rd revised manuscript provisional acceptance January 4, 2024; 4th revised manuscript received January 18, 2024; final acceptance January 26, 2024; preliminary ahead of print version published April 1, 2024.
DOI:10.1306/03212422156

AUTHORS

NOAH MORRIS ~ *Department of Geosciences, University of Arkansas, Fayetteville, Arkansas; nm009@uark.edu*

Noah Morris is a Ph.D. candidate at the University of Arkansas researching the geochemistry of organic-rich shales. He received a B.S. degree in geology from the University of Oklahoma in 2010 and an M.S. degree in geology from the University of Arkansas in 2017. Between receiving his undergraduate and M.S. degrees, he worked for Geosearch Logging and ALS Empirica. He is the corresponding author of this paper.

ADRIANA POTRA ~ *Department of Geosciences, University of Arkansas, Fayetteville, Arkansas; potra@uark.edu*

Adriana Potra specializes in economic ore geology and radiogenic isotope geochemistry, with the main research focus on enhancing the understanding of the geochemistry of ore deposits. As a graduate student at Florida International University, she worked on magmatic-hydrothermal systems. Since joining the University of Arkansas, she has been doing research on constraining the metal source(s) in the Mississippi Valley-type deposits.

JOHN R. SAMUELSEN ~ *Arkansas Archeological Survey, Fayetteville, Arkansas; Department of Anthropology, University of Arkansas, Fayetteville, Arkansas; jsamuel@uark.edu*

John R. Samuelsen is an archeologist and computer specialist at the Arkansas Archeological Survey. He received his B.A. and B.S. degrees at the University of Florida in 2004, his M.A. degree at the University of Arkansas in 2009, and his Ph.D. at the University of Arkansas in 2020. He is further developing the use of lead and strontium isotopes for ancient human sourcing.

ACKNOWLEDGMENTS

This study was funded by US National Science Foundation Grant No. 1952088. Core samples were provided by the Wisconsin Geological and Natural History Survey. Thanks to Erik Pollock, Lindsey

Conaway, and Barry Shaulis for their laboratory assistance in analyses using the ThermoScientific iCAP Q inductively coupled plasma-mass spectrometry (ICP-MS), Nu Plasma multicollector ICP-MS, and Thermo Scientific EA IsoLink isotope ratio MS CN system at the University of Arkansas. Thanks are also extended to Will Hadley, Jackson Copeland, and Alex Goodsuhm for field and laboratory support, as well as Bryan Bottoms and Christophe Simbo for sample collection. Thanks to Ahmed Mansour and anonymous reviewers for their constructive comments.

DATASHARE 186

Tables S1 and S2 are available in an electronic version on the AAPG website (www.aapg.org/datashare) as Datashare 186.

INTRODUCTION

The formation of shale is a complex topic because shales can potentially form in any depositional environment that allows clay-size sediment to settle out of the water column in sufficient quantities, including lacustrine or fluvial settings, deltas, restricted marine settings (e.g., tidal flats and lagoons), and marine settings where the sea floor is below storm-wave base and some high energy environments, such as debris flows (Boggs, 2006; Peng, 2021). Black shales have been interpreted to form in many of these environments, including both shallow and deep marine, which complicates interpreting their depositional environments. To better constrain their depositional history, geochemical analyses using trace element concentrations can be used as paleoredox proxies (Jones and Manning, 1994; Tribovillard et al., 2006; Algeo and Rowe, 2012; Algeo and Li, 2020; Algeo and Liu, 2020; Bennett and Canfield, 2020; Horner et al., 2021).

This study is a geochemical survey of Paleozoic black shales from the midcontinent United States (Figure 1) where their geochemical signatures are compared to infer the conditions of their depositional environments. The samples were selected from Cambrian- to Pennsylvanian-age formations from the Ozark Dome, Ouachita Mountains, and the Cherokee, Forest City, and Illinois Basins (Figure 2). The selection of black shales for this study was based on their diverse spatial and temporal distribution, characterized by high organic content (>5 wt. % total organic carbon [*TOC*]) and metal-rich attributes, as reported by Coveney and Glascock (1989) and Coveney (2003). Additionally, the proximity of these shales to various Mississippi Valley-type (MVT) ore deposits in the midcontinent United States served as an additional criterion, although a detailed examination of the correlation between the shales and MVT deposits falls outside the scope of this paper.

GEOLOGIC SETTING

There were significant tectonic, geographic, and climatic changes to the midcontinent of North America during the Paleozoic Era. During the Cambrian through Devonian, the midcontinent United States was located between ~15° and 30° south of the equator, and much of the region experienced warm to arid climatic conditions during much of that time (Boucot et al., 2013). During the Carboniferous, the craton had migrated to near-equatorial latitudes, becoming subject to more tropical climates (Boucot et al., 2013).

The Ozark Dome, situated in the central part of the study area, is an uplifted area of Precambrian (1.476 ± 0.016 Ga) granite and rhyolite, followed by 1.38-Ga alkaline intrusions and

~1.33-Ga mafic intrusions (Lowell and Young, 1999; Meert and Stuckey, 2002). These igneous rocks outcrop in parts of southeastern Missouri at the St. Francis Mountains. Overlying this granite and rhyolite is a sequence of Cambrian- to Mississippian-age sedimentary rocks. The Ozark Dome is asymmetrical, with the Paleozoic strata dipping less than 1° on the southwestern margin. The eastern margin terminates steeply along fault zones (typically reverse faults) and the Reelfoot rift that separate the Ozark Dome and the Illinois Basin (Chinn and König, 1973; McBride and Nelson, 1999). These fault zones, initiated during the early Middle Devonian, were preceded by the Reelfoot rift, a late Proterozoic to early Cambrian rift zone now buried under Cretaceous and Cenozoic sediments of the northern reaches of the Mississippi Embayment (Ervin and McGinnis, 1975; Devera and Fraunfelter, 1988; Nelson and Zhang, 1991; Parrish and Van Arsdale, 2004; Van Arsdale and Cupples, 2013). The southern Ozark Dome primarily consists of east-striking normal faults with a mixture of northeast-striking, strike-slip faults that formed in association with the Ouachita orogeny (Hudson, 2000). In the Ozark Dome province, the Chattanooga Shale (Devonian) and the Fayetteville Shale (Mississippian) were both sampled and are recognized with formation status in Arkansas, Oklahoma, and Missouri. The Ouachita Mountains are situated along the Ouachita fold-thrust belt, which extends from southwestern Texas and northern Mexico to the southern Appalachian Mountains. The Ouachita Mountains are a result of transpressional orogeny of Laurentia and Gondwana during the early Carboniferous as the Laurentian plate subducted under the Gondwanan plate (Hatcher, 2002; Nance et al., 2010). Laurentia and Gondwana collided along the southern Appalachians, resulting in the Alleghanian orogeny. The collision rotated in a clockwise manner, leading to a "zipper" effect as the sea closed and the orogeny continued along the Ouachita fold-thrust belt (Hatcher, 2002). In response, some foreland basins developed along the northern periphery of the Ouachita fold-thrust belt, such as the Arkoma Basin.

The Ouachita stratigraphy is generally composed of deep-water, turbiditic facies where sandstones and shales are the dominant lithologies (Morris, 1971; Owen and Carozzi, 1986). The sampled Ouachita Mountain stratigraphic units in this study include the Collier Shale (upper Cambrian to Lower Ordovician),

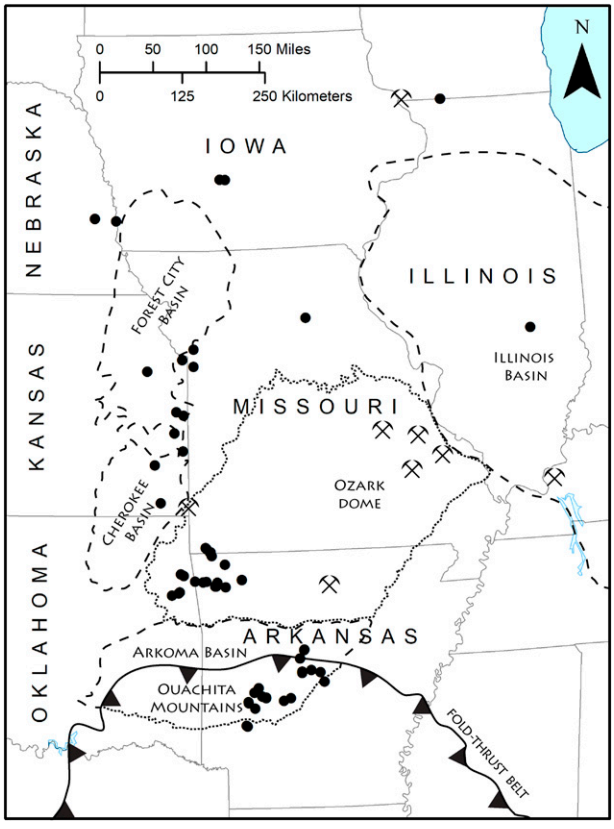

Figure 1. Sample localities (black dots) with basins (dashed lines), uplifts (dotted lines), and the Ouachita fold-thrust belt. Lead–zinc mining districts (crossed picks) are known for epigenetic ore occurrences primarily hosted within carbonate rocks, with potential variability in mineralization relationships to the studied shales.

Mazarn Shale (Lower Ordovician), Womble Shale (Middle to Upper Ordovician), Polk Creek Shale (Upper Ordovician), Stanley Shale (Meramecian to Chesterian Series, Mississippian), Jackfork Sandstone (Morrowan Series, Pennsylvanian), and the Atoka Formation (Atokan Series, Pennsylvanian) (Figure 2). All Ouachita units analyzed in this study were collected from Arkansas where they are recognized with formation lithostratigraphic rank. Although the Collier Shale is the oldest exposed formation in Arkansas, it is not well studied due to its limited exposure and unexposed base (McFarland, 2004). The Jackfork Formation was deposited before the formation of the Arkoma Basin and contains deep-water flysch deposited during the initiation of the orogen, followed by the deposition of the Atoka Formation, which comprises much of the basin's sediment (up to ~7620 m thick) (Morris, 1971; Owen and Carozzi, 1986; McFarland, 2004).

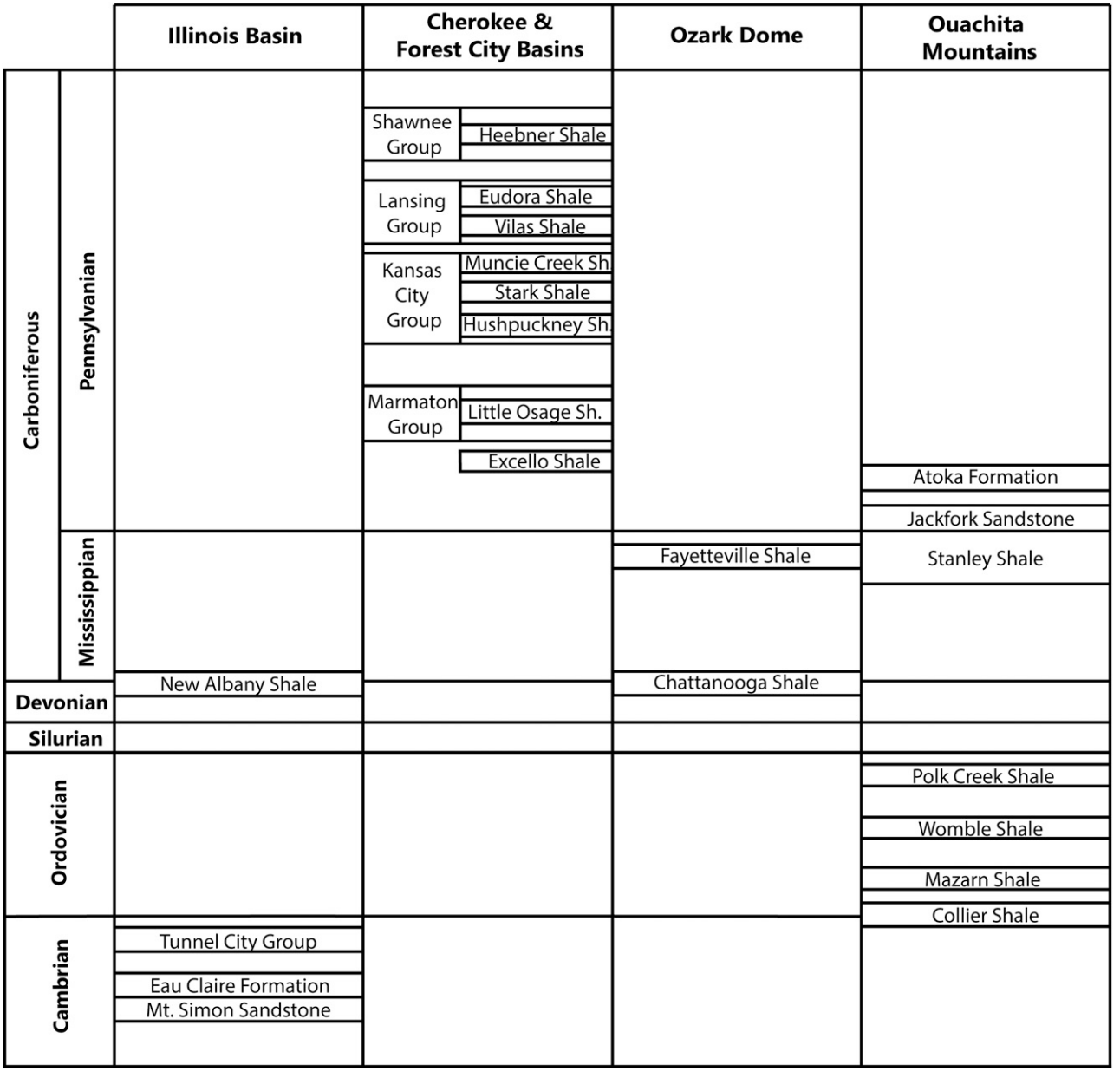

Figure 2. Generalized stratigraphic columns of the sampled shales in the study area. Sh. = Shale.

The Illinois Basin developed because of multiple tectonic events that occurred throughout Precambrian to Cambrian time, as well as in response to the development of the Reelfoot rift and the Rough Creek graben following the breakup of a supercontinent (Klein and Hsui, 1987; Kolata and Nelson, 1990a, b). The basin subsided as an embayment in the cratonic interior where the Paleozoic stratigraphic units generally dip south toward the Reelfoot rift and the Rough Creek graben (Klein and Hsui, 1987; Kolata and Nelson, 1990a, b). During the Carboniferous and Permian, the Illinois Basin subsided further due to compressional stresses on the cratonic interior that occurred in response to the Alleghanian and Ouachita orogenies (Klein and Hsui, 1987; Kolata and Nelson, 1990a, b). Throughout most of the basin, the Mt. Simon Sandstone overlies the Precambrian igneous basement rocks (Sargent, 1990).

The Illinois Basin region is composed of several clastic and carbonate successions, including the Mt. Simon Sandstone (Cambrian), the Eau Claire Formation (Cambrian), the Tunnel City Group (Cambrian), and the New Albany Shale (Devonian). The three Cambrian units were sampled from the northern

margin of the Illinois Basin, and the New Albany was sampled from the central part of the Illinois Basin.

The Cherokee Basin, which spans Oklahoma and Kansas, and the Forest City Basin, which spans Kansas, Missouri, Nebraska, and Iowa, are cratonic basins consisting of a series of clastics and carbonates. These basins are separated by the Bourbon arch and have their axes further west near the Nemaha uplift, which was activated during the middle Carboniferous (Jopling and Cashion, 1959; Anderson and Wells, 1968; Harris, 1985; Leighton and Kolata, 1990; Newell, 1995). The basins have generally been subsiding since the Cambrian but experienced more rapid subsidence during the Pennsylvanian due to intracratonic stresses that occurred in response to the Alleghanian and Ouachita orogenies, similar to the Illinois Basin (Leighton and Kolata, 1990).

The sampled stratigraphic units in the Cherokee and Forest City Basins are all Pennsylvanian in age. Although the lithostratigraphic ranks of these units vary across the states they are found in, these shales are generally referred to as a member within the state they were sampled in. These units include the Excello Shale, the Little Osage Shale Member of the Marmaton Group (Desmoinesian Series), the Hushpuckney, Stark, and Muncie Creek Shale Members of the Kansas City Group (Missourian Series), the Vilas and Eudora Shale of the Lansing Group (Missourian Series), and the Heebner Shale Member of the Shawnee Group (Virgilian Series).

Paleoredox, Paleoproductivity, and Paleosalinity Proxies

In this study, a suite of paleoenvironmental proxies were employed to characterize the geochemical signatures of black shales and to infer the bottom-water conditions at the time of deposition. Specifically, these proxies focus on the V/Cr, Ni/Co, U/Th, and authigenic U (U-Th/3) proxies as evaluated by Jones and Manning (1994), which have demonstrated their reliability for reconstructing paleoredox conditions. The Mo concentration and Mo/*TOC* paleoredox proxies follow the approach of Scott and Lyons (2012), whereas the V/(V+Ni) paleoredox proxy follows Hatch and Leventhal (1992). Additional proxies considered include the basin restriction proxies (Cd/Mo and Co × Mn) of Sweere et al. (2016) and the Sr/Ba paleosalinity proxy of Wei and Algeo (2020). To accompany these proxies, Tyson and Pearson's (1991) thresholds are used to describe the oxygen content of the seawater: anoxic (0.0 ml O_2/L H_2O, H_2S = 0), euxinic (0.0 ml O_2/L H_2O, H_2S > 0), dysoxic (~0.0–2.0 ml O_2/L H_2O), and oxic (>2.0 ml O_2/L H_2O). This study acknowledges that certain conditions, such as elevated thermal maturity, diagenesis, and sedimentation rate, may render specific proxies unsuitable for application in some cases (Klinkhammer and Palmer, 1991; Ardakani et al., 2016; Hood et al., 2018; Algeo and Liu, 2020; Crombez et al., 2020; Mansour et al., 2020; Peng, 2022). However, this study uses a suite of proxies that, when aggregated together, should provide reliable insights into the depositional conditions of the shales.

The elements Mo, V, Ni, Co, Cr, U, and Th hold significant importance as paleoredox proxies in shale geochemical analysis. Uranium predominantly exists as U(VI) in uranyl ions in seawater, with authigenic U enrichment occurring in sediments due to U(VI) to U(IV) reduction (Anderson et al., 1989; Klinkhammer and Palmer, 1991; Crusius et al., 1996; Algeo and Maynard, 2004). Thorium is used as a comparison with U in paleoredox proxies because Th is relatively immobile and typically is found in detrital sediments (Jones and Manning, 1994). Vanadium behaves quasi-conservatively in oxic waters, associating closely with the Mn redox cycle in sediments (Hastings et al., 1996). It can readily be adsorbed on Mn and Fe oxyhydroxides as vanadate (oxidized V) (Calvert and Piper, 1984; Wehrli and Stumm, 1989) and can be reduced to V(IV) under mildly reducing conditions (Emerson and Huested, 1991; Morford and Emerson, 1999). Molybdenum, abundant relative to biological requirements, exhibits conservative distribution and is also easily adsorbed on Mn oxyhydroxides in sediments (Bertine and Turekian, 1973; Crusius et al., 1996). Enrichment of Mo is linked to organic matter abundance, sulfate reduction activity, and sulfide presence (François, 1988; Erickson and Helz, 2000; Vorlicek et al., 2004). Chromium exists as Cr(VI) in oxygenated seawater and is reduced to Cr(III) under anoxic conditions, readily complexing with humic/fulvic acids or adsorbing on Fe and Mn oxyhydroxides (Calvert and Pedersen, 1993). Cobalt appears as the dissolved cation or complexed with humic/fulvic acids in oxic environments, and it forms insoluble CoS in anoxic waters (Huerta-Diaz and Morse, 1992). Nickel behaves as a

micronutrient in oxic marine environments, cycling between the sediment and overlying waters based on the presence of sulfides and Mn oxides (Huerta-Diaz and Morse, 1990, 1992; Morse and Luther, 1999).

For the Co × Mn and Cd/Mo basin restriction proxies, these elements are useful since Mn and Co are actively scavenged from the water column, resulting in their depletion with depth, whereas the distribution of Cd is influenced by phytoplankton uptake and release (Bruland, 1980; Landing and Bruland, 1980; Knauer et al., 1982; Statham and Burton, 1986; Conway and John, 2015; Sweere et al., 2016). In contrast, Mo displays conservative behavior and is not significantly influenced by biological interactions (Emerson and Huested, 1991; Nakagawa et al., 2012). Redox conditions strongly influence the removal pathways of these elements, with Mn becoming more soluble under reducing conditions and Co, Cd, and Mo being efficiently sequestered into sediments (Huerta-Diaz and Morse, 1992; Erickson and Helz, 2000; Vorlicek et al., 2004; Tribovillard et al., 2006; Little et al., 2015). The behavior of Mo in euxinic waters makes it a robust paleoredox proxy, as previously discussed (Crusius et al., 1996; Algeo and Lyons, 2006; Algeo and Tribovillard, 2009; Scott and Lyons, 2012).

In the Sr/Ba proxy, Sr primarily originates from continental weathering and enters the ocean through rivers, whereas Ba exhibits a more complex behavior, influenced by sources like hydrothermal activity and biogenic productivity, and is scavenged by particles in the water column (Godderis and Veizer, 2000; Krabbenhöft et al., 2010). Barium's higher affinity for particulate matter makes it more abundant in freshwater and detrital sediments, rendering it a crucial indicator of freshwater input, whereas Sr is more commonly found in marine-precipitated minerals as a substitution for Ca^{2+} (Roden et al., 2002; Das and Krishnaswami, 2006; Vetter et al., 2017). The Sr/Ba ratio is affected by changes in seawater salinity, with high salinity potentially leading to a higher Sr/Ba ratio due to reduced particle scavenging (Wei and Algeo, 2020).

SAMPLING AND METHODOLOGY

Sample Collection and Preparation

Sixty-nine shale samples from 21 stratigraphic units from across the midcontinent United States were used in this study (Figure 2). Nearly all samples were collected from outcrops in Arkansas, Iowa, Kansas, Missouri, Nebraska, and Oklahoma (Figure 1; Table 1). All samples came from exposures where fresh samples were able to be collected by removing as much of the exposed surface as possible using conventional hand tools to obtain the least weathered samples from behind the outcrop exposure. When available, type sections or type localities were chosen for sampling. The type localities of the following shales were sampled during August 2020: Stark (near Stark, Neosho County, Kansas) (Moore, 1932; Jewett, 1933), Hushpuckney (railway cut, center north side, Sec. 13, T19S, R23E, Miami County, Kansas) (Moore, 1932), Muncie Creek (Muncie Creek, east of Muncie, Kansas, in the southern part of Wyandotte County, Kansas) (Moore, 1932), and Fayetteville (near Fayetteville, Washington County, Arkansas) (Simonds, 1891). The Excello Shale was sampled approximately 1.5 miles from the type section described in Searight (1955) (NW/4 Sec. 30, T56N, R14W, 2.6 mi west of US Highway 63, west of Excello, Macon County, Missouri, in the highwall of a coal strip mine pit).

Several sampled localities were chosen because they had previously been described (see Table 1). Selected samples of the Collier, Mazarn, Womble, Polk Creek, Chattanooga, Stanley, and Fayetteville Shales, as well as the Jackfork Sandstone, have been previously analyzed by Simbo et al. (2019) in an effort to constrain depositional conditions using geochemical techniques. However, this study uses what is considered a more accurate geochemical processing method (full digestion rather than partial digestion) and analyzes additional elements for a more thorough geochemical investigation.

Four additional samples originated from the Commonwealth Edison UPH-1 core in northern Illinois (Wisconsin Geological and Natural History Survey [WGNHS] identification number [ID] 33000331) and one additional sample from the WGNHS Hwy A Quarry 2 core from southern Wisconsin (WGNHS ID 25000529). The core samples were donated by the Wisconsin Geological and Natural History Survey to provide additional geochemical data for shales in the northern Mississippi River Valley. Samples from these cores include the Eau Claire, Tunnel City, and Mt. Simon units and have been part of a previous Pb isotope study (Doe et al., 1983). One other sample, representing the New Albany Shale, originated from

well cuttings from the Morris 1 well drilled by Ceja Corporation in 2012 in Shelby County, Illinois (API 12-173-24362). One of the authors was present at the time of drilling and collected this sample after cleaning it from water-based drilling mud. In sum, seven shales have only one sample from each (Mt. Simon and Tunnel City [Cambrian]; Collier [Cambrian–Ordovician]; New Albany [Devonian], and Muncie Creek, Stark, and Vilas [Pennsylvanian]), which cannot be used to draw inferences, but they can be used to compare with the other temporally and spatially related shale units in this study.

Samples were rinsed with deionized water, dried, and then powdered in an alumina-ceramic dish using a Spex SamplePrep Shatterbox. All further processing of the samples was conducted in a class 100 cleanroom at the University of Arkansas to reduce potential environmental contamination and all labware used for chemical processing of the samples was acid cleaned to minimize possible contamination. All acids used in the chemical processing were previously distilled in dedicated HNO_3 and HCl Savillex DST-1000 acid purification systems.

TOC

The *TOC* was evaluated for its use in the Mo/*TOC* paleoredox proxy. Dry, powdered samples were weighed on a Sartorius ISO 9001 microbalance and placed within a tin capsule. The samples were analyzed on a Thermo Scientific EA IsoLink isotope ratio mass spectrometry (IRMS) carbon-nitrogen system (includes Flash IRMS elemental analyzer, Delta V IRMS, and Conflo IV universal interface) at the University of Arkansas Stable Isotope Laboratory. The samples were calibrated with 27 internal silty soil standard samples (averaging 2.19 wt. %; standard deviation (σ) = 0.071).

Sample Digestion

One hundred milligrams of powder from each sample were weighed and placed in the polyfluoroalkyl (PFA) liner of a Parr acid-digestion vessel (model number 4749). Two milliliters of reverse aqua regia (3 parts distilled HNO_3:1 part distilled HCl) were added to each sample in a laminar flow fume hood. Two milliliters of concentrated HF were also added to each sample and left uncovered for 10 min to vent volatile gases. The samples in the Parr liners were inserted into the Parr acid digestion vessels and tightened. The vessels were placed in a Lindberg Blue M 828 oven and heated to 200°C for 8 hr. The vessels were allowed to cool for 24 hr, and the liners were extracted and placed in a laminar flow fume hood in the class 100 clean room. The solution in each liner was pipetted into a clean 30 ml PFA vial and dried at 90°C. Each sample had 4 ml of distilled HNO_3 added and was then heated to 150°C for 8 hr while tightly capped and subsequently dried at 90°C. Four milliliters of distilled HCl were then added and heated to 150°C for 8 hr while capped and then dried at 90°C. This process of adding HNO_3 and HCl was repeated once more. After each addition of heat, the samples were cooled to room temperature, and after each addition of acid, the samples were allowed to remain uncovered for 10 min to remove any volatile gases.

Elemental Concentrations

The dried, digested samples were redissolved in 2 ml of 2% HNO_3 at 150°C for 1 hr. A volume of 0.1 ml of each sample solution was transferred to clean 5-ml centrifuge tubes and diluted with 2.9 ml of 2% HNO_3. The samples were analyzed on a Thermo Scientific iCAP Q inductively coupled plasma-mass spectrometry (ICP-MS) instrument at the University of Arkansas Trace Element and Radiogenic Isotope Laboratory. The samples were analyzed for elements associated with detrital sediment input and redox-sensitive trace elements. Concentrations are reported on a whole rock basis (part per million) in Table 2 and Table S1 (supplementary material available as AAPG Datashare 186 at www.aapg.org/datashare) (with standard deviations in Table S2, supplementary material available as AAPG Datashare 186 at www.aapg.org/datashare). In addition, two sets of ICP-MS multielement solution standards were made using 10 ppm Inorganic Ventures IV-ICP-MS-71B and 10 ppm high-purity standards ICP-MS-68A-A-100 diluted to multiple concentrations (500 ppb [$\sigma = 7.73 \times 10^{-1}$], 100 ppb [$\sigma = 3.16 \times 10^{\circ}$], 50 ppb [$\sigma = 2.32 \times 10^{\circ}$], 10 ppb [$\sigma = 5.34 \times 10^{-1}$], 5 ppb [$\sigma = 4.09 \times 10^{-1}$], 1 ppb [$\sigma = 5.59 \times 10^{-1}$], and 10‰ [$\sigma = 7.95 \times 10^{-1}$]). Seven duplicate samples and five replicate samples were also analyzed; these samples were chosen based on age, number of samples for each shale, and total mass of each sample available.

Table 1. Sampled Units and Their Localities

Formation	Member	Sample ID	Age	Locality	Coordinates	Basin/Province
Oread	Heebner	9 Heebner	Pennsylvanian	Lawrence, KS	38.956984, −95.319143	Cherokee–Forest City
Oread	Heebner	13 Heebner*	Pennsylvanian	Plattsmouth, NE	40.987332, −95.860284	Cherokee–Forest City
Stanton	Eudora	15 Eudora*	Pennsylvanian	Gretna, NE	41.020087, −96.249668	Cherokee–Forest City
Stanton	Eudora	21 Eudora†	Pennsylvanian	Kansas City, MO	39.243871, −94.495858	Cherokee–Forest City
Vilas	–	15 Vilas*	Pennsylvanian	Gretna, NE	41.020087, −96.249668	Cherokee–Forest City
Iola	Muncie Creek	11-1 Muncie Creek‡	Pennsylvanian	Muncie, KS	39.105029, −94.696840	Cherokee–Forest City
Iola	Muncie Creek	11-2 Muncie Creek‡	Pennsylvanian	Muncie, KS	39.105029, −94.696840	Cherokee–Forest City
Dennis	Stark	2 Stark‡§	Pennsylvanian	Stark, KS	37.688367, −95.197550	Cherokee–Forest City
Swope	Hushpuckney	5 Hushpuckney§	Pennsylvanian	Mound City, KS	38.115926, −94.851675	Cherokee–Forest City
Swope	Hushpuckney	6 Hushpuckney¶	Pennsylvanian	Lacygne, KS	38.356363, −94.687232	Cherokee–Forest City
Swope	Hushpuckney	8 Hushpuckney‡	Pennsylvanian	Fontana, KS	38.402554, −94.813937	Cherokee–Forest City
Swope	Hushpuckney	20 Hushpuckney†	Pennsylvanian	Kansas City, MO	39.013522, −94.502805	Cherokee–Forest City
Fort Scott	Little Osage	3 Little Osage¶	Pennsylvanian	Fort Scott, KS	37.873814, −94.704829	Cherokee–Forest City
Stephens Forest	Little Osage	16A Little Osage†	Pennsylvanian	Van Meter, IA	41.537628, −93.973555	Cherokee–Forest City
Excello	–	1 Excello#	Pennsylvanian	Oswego, KS	37.175243, −95.102767	Cherokee–Forest City
Excello	–	17 Excello**	Pennsylvanian	Booneville, IA	41.532000, −93.872849	Cherokee–Forest City
Excello	–	19 Excello††	Pennsylvanian	Excello, MO	39.636663, −92.492791	Cherokee–Forest City
Atoka	Upper	UA1Sh	Pennsylvanian	Morrilton, AR	35.156467, −92.719217	Arkoma Basin
Atoka	Lower	LA1Sh	Pennsylvanian	Perry, AR	35.039533, −92.795967	Arkoma Basin
Atoka	Lower	LA2Sh	Pennsylvanian	Mt. Moriah, AR	34.135717, −93.700383	Arkoma Basin
Atoka	–	Atoka 2	Pennsylvanian	Morrilton, AR	35.148467, −92.720383	Arkoma Basin
Jackfork	Upper	UJ1Sh	Pennsylvanian	Williams Junction, AR	34.857433, −92.767617	Ouachita Mtns
Jackfork	Upper	UJ2Sh	Pennsylvanian	Mt. Moriah, AR	34.147483, −93.715833	Ouachita Mtns
Jackfork	Middle	MJ1	Pennsylvanian	Pinnacle, AR	34.843100, −92.462917	Ouachita Mtns
Jackfork	Middle	MJ2	Pennsylvanian	Northpoint, AR	34.876500, −92.614400	Ouachita Mtns
Jackfork	Lower	LJ1	Pennsylvanian	Williams Junction, AR	34.840783, −92.767917	Ouachita Mtns
Fayetteville	Lower	FS1L	Mississippian	Weddington, AR	36.099378, −94.395122	Ozark Dome
Fayetteville	Upper	FS2U	Mississippian	Fayetteville, AR	36.042400, −94.191200	Ozark Dome
Fayetteville	–	FS3	Mississippian	Fayetteville, AR	36.045778, −94.180353	Ozark Dome
Fayetteville	–	FS4	Mississippian	Fayetteville, AR	36.040833, −94.174528	Ozark Dome
Fayetteville	Lower	FS6L	Mississippian	Fayetteville, AR	36.092586, −94.152103	Ozark Dome
Fayetteville	Lower	FS7L	Mississippian	Elkins, AR	36.027800, −94.012700	Ozark Dome
Fayetteville	Upper	FS8UU	Mississippian	Huntsville, AR	36.119692, −93.740072	Ozark Dome
Fayetteville	Upper	FS9LU	Mississippian	Huntsville, AR	36.119719, −93.739983	Ozark Dome
Fayetteville	Lower	FS10L	Mississippian	Huntsville, AR	36.119861, −93.739386	Ozark Dome
Fayetteville	–	FS11	Mississippian	Fayetteville, AR	36.070272, −94.167028	Ozark Dome
Stanley	–	Stanley 1	Mississippian	Hot Springs, AR	34.505850, −92.969133	Ouachita Mtns
Stanley	–	Stanley 2	Mississippian	Hot Springs, AR	34.469300, −93.088067	Ouachita Mtns
Stanley	–	Stanley 3	Mississippian	Hot Springs, AR	34.469300, −93.088067	Ouachita Mtns
Stanley	–	Stanley 4	Mississippian	Glenwood, AR	34.375567, −93.566250	Ouachita Mtns
Chattanooga	–	CS1	Devonian	Tahlequah, OK	35.926292, −94.927411	Ozark Dome
Chattanooga	–	CS2	Devonian	Proctor, OK	35.955250, −94.814236	Ozark Dome

(*continued*)

Table 1. Continued

Formation	Member	Sample ID	Age	Locality	Coordinates	Basin/Province
Chattanooga	–	CS3	Devonian	Proctor, OK	35.967667, −94.791722	Ozark Dome
Chattanooga	–	CS4	Devonian	Kansas, OK	36.211103, −94.771083	Ozark Dome
Chattanooga	–	CS5	Devonian	Flint Creek, OK	36.190972, −94.721250	Ozark Dome
Chattanooga	–	CS6	Devonian	Siloam Springs, AR	36.112311, −94.533322	Ozark Dome
Chattanooga	–	CS7	Devonian	Savoy, AR	36.106653, −94.339125	Ozark Dome
Chattanooga	–	CS8	Devonian	Jane, MO	36.561322, −94.343603	Ozark Dome
Chattanooga	–	CS9	Devonian	Jane, MO	36.546711, −94.327603	Ozark Dome
Chattanooga	Lower	CS10B	Devonian	Pineville, MO	36.504072, −94.258875	Ozark Dome
Chattanooga	–	CS11	Devonian	Bella Vista, AR	36.496800, −94.265400	Ozark Dome
Chattanooga	–	CS12	Devonian	Bella Vista, AR	36.450400, −94.240300	Ozark Dome
Chattanooga	–	CS13	Devonian	Rogers, AR	36.331836, −94.020014	Ozark Dome
New Albany	–	Ceja Corp Morris #1	Devonian	Neoga, IL	39.337800, −88.516500	Illinois Basin
Polk Creek	–	Polk Creek 1	Ordovician	Little Rock, AR	34.715317, −92.401217	Ouachita Mtns
Polk Creek	–	PC1	Ordovician	Washita, AR	34.652783, −93.500333	Ouachita Mtns
Womble	–	Womble 1	Ordovician	Crystal Springs, AR	34.514117, −93.381017	Ouachita Mtns
Womble	–	Womble 2	Ordovician	Norman, AR	34.450400, −93.670417	Ouachita Mtns
Womble	–	Womble 3	Ordovician	Little Rock, AR	34.715317, −92.401217	Ouachita Mtns
Mazarn	–	Mazarn 1	Ordovician	Mt. Ida, AR	34.590150, −93.572117	Ouachita Mtns
Mazarn	–	Mazarn 2	Ordovician	Mt. Ida, AR	34.539200, −93.444950	Ouachita Mtns
Mazarn	–	Mazarn 3	Ordovician	Crystal Springs, AR	34.521867, −93.377283	Ouachita Mtns
Mazarn	–	Mazarn 4	Ordovician	Norman, AR	34.465617, −93.676983	Ouachita Mtns
Collier	–	Collier CS1	Camb.–Ordo.	Mt. Ida, AR	34.523183, −93.395700	Ouachita Mtns
Tunnel City	–	UPH-1-658‡‡	Cambrian	Winslow, IL	42.504940, −89.852062	Illinois Basin
Eau Claire	–	HwyA-2-520	Cambrian	Hollandale, WI	42.877445, −89.872223	Illinois Basin
Eau Claire	–	UPH-1-853‡‡	Cambrian	Winslow, IL	42.504940, −89.852062	Illinois Basin
Eau Claire	–	UPH-1-977‡‡	Cambrian	Winslow, IL	42.504940, −89.852062	Illinois Basin
Mt. Simon	–	UPH-1-1363‡‡	Cambrian	Winslow, IL	42.504940, −89.852062	Illinois Basin

Abbreviations: AR = Arkansas; Camb. = Cambrian; Corp = Corporation; HwyA = Highway A; IA = Iowa; ID = identification; IL = Illinois; KS = Kansas; MO = Missouri; Mtns = Mountains; NE = Nebraska; OK = Oklahoma; Ordo. = Ordovician; WI = Wisconsin.

*Locality previously described in Burchett (1971).

†Locality previously described in Morris, (2014).

‡Type locality.

§Locality previously described in Ece, (1985; 1987).

¶Locality previously described in Nestell et al., (2016).

#Locality previously described in Keroher and others (1966).

**Locality previously described in Cubitt, (1979).

††Locality previously described in Buchanan and McCauley, (2010).

‡‡Locality previously described in Doe et al., (1983).

Table 2. Concentrations and Proxy Values of Samples

Shale Name	Sample ID	Age	V, ppm	Cr, ppm	Mn, ppm	Co, ppm	Ni, ppm	Sr, ppm	Mo, ppm	Cd, ppm	Ba, ppm	Th, ppm	U, ppm	*TOC*, wt. %	Mo/*TOC*	V/(V+Ni)	U/Th	U-(Th/3)	V/Cr	Ni/Co	Cd/Mo	Co × Mn	Sr/Ba
Heebner	9 Heebner	Pennsylvanian	891.5	567.7	183.2	10.3	192.7	78.7	93.9	35.3	218.9	8.7	15.9	14.78	6.4	0.82	1.8	13.0	1.6	18.6	0.38	0.19	0.4
Heebner	13 Heebner	Pennsylvanian	2111.8	314.1	214.8	9.7	241.0	142.9	274.7	99.8	301.7	8.3	40.8	17.68	15.5	0.90	4.9	38.1	6.7	24.9	0.36	0.21	0.5
Heebner	13 Heebner (R)	Pennsylvanian	2292.8	336.7	232.7	10.4	256.4	160.5	304.7	108.6	290.9	9.5	46.0	n.d.	n.d.	0.90	4.9	42.8	6.8	24.8	0.36	0.24	0.6
Eudora	15 Eudora	Pennsylvanian	792.9	549.1	134.1	40.5	683.7	92.0	28.6	30.9	598.3	10.7	33.9	10.02	2.8	0.54	3.2	30.3	1.4	16.9	1.08	0.54	0.2
Eudora	21 Eudora	Pennsylvanian	995.4	358.8	210.6	10.4	354.6	114.9	109.8	107.4	213.1	9.9	26.4	18.90	5.8	0.74	2.7	23.1	2.8	34.0	0.98	0.22	0.5
Vilas	15 Vilas	Pennsylvanian	65.1	79.2	225.4	14.3	43.4	225.9	4.1	0.2	242.3	6.8	6.8	5.07	0.8	0.60	1.0	4.5	0.8	3.0	0.05	0.32	0.9
Muncie Creek	11-1 Muncie Creek	Pennsylvanian	2427.8	532.5	84.2	6.7	345.1	59.3	261.0	7.2	332.4	9.4	48.7	28.06	9.3	0.88	5.2	45.6	4.6	51.3	0.03	0.06	0.2
Muncie Creek	11-2 Muncie Creek	Pennsylvanian	1929.1	425.7	111.2	7.4	294.4	57.9	184.1	19.8	196.2	7.9	28.1	23.07	8.0	0.87	3.6	25.4	4.5	39.7	0.11	0.08	0.3
Stark	2 Stark	Pennsylvanian	184.7	510.5	93.2	7.8	185.4	390.1	21.6	2.0	160.4	4.6	29.4	12.95	1.7	0.50	6.4	27.9	0.4	23.7	0.09	0.07	2.4
Hushpuckney	5 Hushpuckney	Pennsylvanian	101.8	148.0	180.2	11.8	114.8	80.3	6.9	6.3	195.1	11.6	8.5	3.80	1.8	0.47	0.7	4.7	0.7	9.7	0.92	0.21	0.4
Hushpuckney	6 Hushpuckney	Pennsylvanian	567.8	705.3	143.9	8.7	234.5	297.1	44.7	16.1	145.2	8.9	39.6	15.49	2.9	0.71	4.5	36.6	0.8	27.0	0.36	0.12	2.0
Hushpuckney	8 Hushpuckney	Pennsylvanian	2951.9	1143.1	81.1	7.2	406.7	61.5	260.7	68.8	333.9	5.2	32.6	37.01	7.0	0.88	6.3	30.9	2.6	56.2	0.26	0.06	0.2
Hushpuckney	8 Hushpuckney (D)	Pennsylvanian	2993.2	1139.7	80.2	7.1	405.5	68.6	269.7	76.0	224.6	5.2	40.7	n.d.	n.d.	0.88	7.8	39.0	2.6	57.4	0.28	0.06	0.3
Hushpuckney	20 Hushpuckney	Pennsylvanian	699.0	869.1	143.4	10.6	291.2	104.2	73.4	26.7	133.3	9.8	24.6	21.75	3.4	0.71	2.5	21.4	0.8	27.5	0.36	0.15	0.8
Little Osage	3 Little Osage	Pennsylvanian	592.5	1282.6	53.8	7.1	383.1	106.9	27.6	3.6	298.2	8.6	19.2	32.41	0.9	0.61	2.2	16.3	0.5	54.2	0.13	0.04	0.4
Little Osage	16A Little Osage	Pennsylvanian	2811.1	698.7	196.4	10.0	191.0	88.0	1.3	1.0	258.3	9.9	36.0	6.98	0.2	0.94	3.6	32.7	4.0	19.1	0.78	0.20	0.3
Excello	1 Excello	Pennsylvanian	227.1	343.7	91.4	5.7	258.7	59.6	11.0	3.3	250.9	8.6	12.3	10.74	1.0	0.47	1.4	9.4	0.7	45.2	0.30	0.05	0.2
Excello	17 Excello	Pennsylvanian	5184.9	883.9	69.4	7.7	654.0	94.8	7.0	128.8	382.5	9.2	38.9	14.06	0.5	0.89	4.2	35.8	5.9	85.5	18.40	0.05	0.2
Excello	19 Excello	Pennsylvanian	187.6	565.7	107.3	7.2	350.9	49.3	30.2	5.1	223.7	8.4	21.0	21.73	1.4	0.35	2.5	18.2	0.3	48.7	0.17	0.08	0.2
Atoka	UA1Sh	Pennsylvanian	120.1	89.6	678.4	14.2	37.9	74.9	0.6	0.3	240.8	4.3	1.3	1.79	0.3	0.76	0.3	−0.1	1.3	2.7	0.50	0.97	0.3
Atoka	LA1Sh	Pennsylvanian	168.1	119.1	91.8	5.5	35.7	57.2	0.6	0.3	380.0	3.6	1.2	0.92	0.6	0.82	0.3	0.0	1.4	6.4	0.45	0.05	0.2
Atoka	LA2Sh	Pennsylvanian	127.6	87.7	380.9	15.5	43.4	66.7	0.4	0.2	353.3	5.8	1.4	0.93	0.5	0.75	0.2	−0.6	1.5	2.8	0.50	0.59	0.2
Atoka	LA2Sh (D)	Pennsylvanian	126.2	89.0	377.6	15.4	43.2	67.0	0.4	0.2	357.6	6.3	1.5	n.d.	n.d.	0.75	0.2	−0.6	1.4	2.8	0.52	0.58	0.2
Atoka	Atoka 2	Pennsylvanian	134.0	96.7	426.6	14.6	43.2	66.2	0.5	0.2	313.8	5.2	1.2	0.91	0.5	0.76	0.2	−0.5	1.4	3.0	0.40	0.62	0.2
Jackfork	UJ1Sh	Pennsylvanian	126.0	96.4	86.6	8.7	43.0	54.6	0.3	0.2	187.4	8.5	1.8	0.99	0.3	0.75	0.2	−1.0	1.3	5.0	0.66	0.08	0.3
Jackfork	UJ2Sh	Pennsylvanian	89.3	76.5	404.8	11.5	40.3	81.1	0.8	0.4	274.1	6.1	1.9	2.65	0.3	0.69	0.3	−0.2	1.2	3.5	0.45	0.47	0.3
Jackfork	UJ2Sh (D)	Pennsylvanian	n.d.	n.d.	n.d.	n.d.	n.d.	n.d.	n.d.	n.d.	n.d.	n.d.	n.d.	2.59	n.d.	n.d.	n.d.	n.d.	n.d.	n.d.	n.d.	n.d.	n.d.
Jackfork	MJ1	Pennsylvanian	146.1	128.9	67.5	5.6	44.3	64.5	0.7	0.4	410.1	9.1	1.8	0.80	0.9	0.77	0.2	−1.2	1.1	7.9	0.57	0.04	0.2
Jackfork	MJ2	Pennsylvanian	111.1	90.9	421.2	14.3	47.1	43.5	0.4	0.3	251.1	7.4	1.5	0.80	0.5	0.70	0.2	−1.0	1.2	3.3	0.68	0.60	0.2
Jackfork	LJ1	Pennsylvanian	137.0	97.6	193.2	9.2	31.7	31.0	0.5	0.4	135.8	3.3	0.9	0.99	0.5	0.81	0.3	−0.2	1.4	3.4	0.92	0.18	0.2
Fayetteville	FS1L	Mississippian	197.8	582.0	90.7	8.1	107.5	109.6	10.7	3.3	299.0	11.7	7.8	7.38	1.4	0.65	0.7	3.9	0.3	13.3	0.31	0.07	0.4
Fayetteville	FS2U	Mississippian	212.4	164.3	328.6	16.7	61.2	127.4	0.8	0.7	212.7	13.1	2.6	1.48	0.5	0.78	0.2	−1.8	1.3	3.7	0.85	0.55	0.6
Fayetteville	FS3	Mississippian	162.5	391.6	280.8	11.0	105.1	137.7	3.1	0.5	161.5	11.0	4.4	5.33	0.6	0.61	0.4	0.7	0.4	9.6	0.15	0.31	0.9
Fayetteville	FS4	Mississippian	236.7	214.6	59.9	11.8	65.2	91.5	1.4	0.5	187.6	11.0	2.5	1.77	0.8	0.78	0.2	−1.2	1.1	5.5	0.33	0.07	0.5
Fayetteville	FS6L	Mississippian	234.1	536.4	260.6	9.1	122.5	242.8	12.3	2.2	105.2	9.7	9.8	8.44	1.5	0.66	1.0	6.6	0.4	13.5	0.18	0.24	2.3
Fayetteville	FS7L	Mississippian	285.9	654.4	45.8	3.6	75.3	100.5	9.2	0.7	288.5	13.3	7.2	7.03	1.3	0.79	0.5	2.8	0.4	21.1	0.08	0.02	0.3
Fayetteville	FS7L (D)	Mississippian	n.d.	n.d.	n.d.	n.d.	n.d.	n.d.	n.d.	n.d.	n.d.	n.d.	n.d.	7.05	n.d.	n.d.	n.d.	n.d.	n.d.	n.d.	n.d.	n.d.	n.d.
Fayetteville	FS8UU	Mississippian	43.8	51.0	388.6	5.2	20.8	53.1	0.2	1.1	85.7	5.4	1.4	0.45	0.4	0.68	0.3	−0.4	0.9	4.0	6.55	0.20	0.6
Fayetteville	FS9LU	Mississippian	60.2	76.3	1268.5	8.0	27.27	117.3	0.2	0.3	128.0	8.1	1.7	1.10	0.2	0.69	0.2	−1.0	0.8	3.4	1.30	1.01	0.9
Fayetteville	FS10L	Mississippian	159.2	169.0	210.0	14.5	49.9	120.4	0.4	0.1	263.5	17.0	2.6	0.70	0.6	0.76	0.2	−3.1	0.9	3.4	0.35	0.31	0.5
Fayetteville	FS11	Mississippian	296.9	486.1	114.3	6.2	68.6	195.1	10.5	12.4	321.4	11.5	14.0	6.08	1.7	0.81	1.2	10.2	0.6	11.0	1.19	0.07	0.6
Stanley	Stanley 1	Mississippian	103.1	62.8	460.9	9.8	25.6	44.0	0.5	0.2	421.3	7.3	1.6	0.69	0.7	0.80	0.2	−0.8	1.6	2.6	0.39	0.45	0.1
Stanley	Stanley 2	Mississippian	51.6	44.8	344.5	9.0	18.3	38.1	0.5	0.2	264.0	4.9	1.5	0.23	1.9	0.74	0.3	−0.1	1.2	2.0	0.54	0.31	0.1
Stanley	Stanley 3	Mississippian	132.3	80.4	295.1	7.5	26.8	34.0	0.3	0.2	455.1	7.5	1.4	0.67	0.4	0.83	0.2	−1.2	1.6	3.6	0.58	0.22	0.1
Stanley	Stanley 4	Mississippian	121.1	79.2	306.3	14.0	34.4	111.5	0.2	0.3	798.3	20.0	3.4	0.29	0.8	0.78	0.2	−3.3	1.5	2.5	0.17	0.43	0.1
Stanley	Stanley 4 (D)	Mississippian	104.3	63.9	249.8	11.2	28.5	70.9	0.2	0.2	414.6	8.3	1.8	n.d.	n.d.	0.79	0.2	−1.0	1.6	2.6	0.70	0.28	0.2

(*continued*)

Table 2. Continued

Shale Name	Sample ID	Age	V, ppm	Cr, ppm	Mn, ppm	Co, ppm	Ni, ppm	Sr, ppm	Mo, ppm	Cd, ppm	Ba, ppm	Th, ppm	U, ppm	*TOC*, wt. %	Mo/*TOC*	V/(V+Ni)	U/Th	U-(Th/3)	V/Cr	Ni/Co	Cd/Mo	Co × Mn	Sr/Ba
Chattanooga	CS1 Chattanooga	Devonian	191.0	81.2	843.3	24.3	77.8	46.0	107.1	1.0	378.5	9.7	40.4	7.60	14.1	0.71	4.2	37.2	2.4	3.2	0.01	2.05	0.1
Chattanooga	CS1 Chattanooga (D)	Devonian	n.d.	n.d.	n.d.	n.d.	n.d.	n.d.	n.d.	n.d.	n.d.	n.d.	n.d.	7.66	n.d.	n.d.	n.d.	n.d.	n.d.	n.d.	n.d.	n.d.	n.d.
Chattanooga	CS2	Devonian	167.0	75.0	67.0	4.1	49.0	43.9	56.5	0.4	351.9	12.5	21.4	3.63	15.6	0.77	1.7	17.3	2.2	12.1	0.01	0.03	0.1
Chattanooga	CS3	Devonian	144.0	67.5	160.8	11.0	46.8	43.4	30.3	0.7	92.2	10.4	15.9	3.44	8.8	0.75	1.5	12.5	2.1	4.2	0.02	0.18	0.5
Chattanooga	CS4	Devonian	116.6	72.1	226.3	12.2	44.6	39.3	18.5	1.3	302.9	12.7	12.2	3.43	5.4	0.72	1.0	7.9	1.6	3.7	0.07	0.28	0.1
Chattanooga	CS5	Devonian	136.2	81.2	136.4	12.8	48.9	42.3	17.6	0.5	337.8	12.9	11.7	3.66	4.8	0.74	0.9	7.4	1.7	3.8	0.03	0.17	0.1
Chattanooga	CS6	Devonian	724.7	214.1	155.2	13.7	63.4	63.8	8.3	0.5	360.3	12.3	17.4	1.91	4.3	0.92	1.4	13.3	3.4	4.6	0.06	0.21	0.2
Chattanooga	CS7	Devonian	214.5	90.6	280.2	26.7	64.1	55.5	62.0	0.9	317.8	10.7	31.0	4.80	12.9	0.77	2.9	27.5	2.4	2.4	0.01	0.75	0.2
Chattanooga	CS7 (R)	Devonian	217.2	91.0	283.3	26.8	64.2	57.8	63.4	0.9	327.5	11.1	32.4	n.d.	n.d.	0.77	2.9	28.7	2.4	2.4	0.01	0.76	0.2
Chattanooga	CS8	Devonian	158.7	91.5	241.9	14.1	45.8	56.6	5.3	0.09	417.4	13.6	6.7	2.30	2.3	0.78	0.5	2.1	1.7	3.3	0.02	0.34	0.1
Chattanooga	CS9	Devonian	139.3	85.0	435.4	17.4	56.8	60.1	11.5	0.1	217.0	13.6	7.0	2.50	4.6	0.71	0.5	2.4	1.6	3.3	0.01	0.76	0.3
Chattanooga	CS10B	Devonian	189.0	102.7	88.5	22.0	64.8	58.3	12.1	0.2	497.2	14.9	15.3	2.92	4.2	0.74	1.0	10.3	1.8	2.9	0.01	0.19	0.1
Chattanooga	CS11	Devonian	172.2	95.5	253.4	16.4	62.4	58.9	7.8	0.1	433.8	14.5	9.6	2.87	2.7	0.73	0.7	4.8	1.8	3.8	0.02	0.42	0.1
Chattanooga	CS12	Devonian	208.6	101.2	244.9	17.3	63.6	63.0	9.9	0.3	233.8	14.9	10.5	2.47	4.0	0.77	0.7	5.5	2.1	3.7	0.03	0.42	0.3
Chattanooga	CS13	Devonian	108.0	81.9	211.4	11.6	42.5	55.1	1.1	0.09	343.3	14.6	6.4	1.93	0.6	0.72	0.4	1.6	1.3	3.7	0.08	0.24	0.2
New Albany	Ceja Corp Morris #1	Devonian	154.0	69.8	220.1	25.0	59.0	46.6	42.4	0.8	213.9	5.6	12.6	5.72	7.4	0.72	2.2	10.7	2.2	2.4	0.02	0.55	0.2
New Albany	Ceja Corp Morris #1 (R)	Devonian	146.9	66.7	210.6	23.7	56.7	44.9	39.8	0.7	202.9	5.1	11.5	n.d.	n.d.	0.72	2.2	9.8	2.2	2.4	0.02	0.50	0.2
Polk Creek	Polk Creek 1	Ordovician	474.1	42.7	11.1	0.03	3.9	3.1	3.3	0.04	177.5	1.8	2.6	0.23	14.1	0.99	1.4	2.0	11.1	159.0	0.01	0.00	0.0
Polk Creek	Polk Creek 1 (D)	Ordovician	488.2	43.6	11.2	0.03	4.1	3.3	6.9	0.06	182.0	2.0	2.7	n.d.	n.d.	0.99	1.3	2.0	11.2	160.0	0.01	0.00	0.0
Polk Creek	PC1	Ordovician	464.5	19.6	19.7	0.3	14.9	9.8	16.9	0.1	134.6	1.6	5.8	2.27	7.4	0.97	3.7	5.2	23.7	59.2	0.01	0.00	0.1
Polk Creek	PC1 (R)	Ordovician	466.5	19.6	19.9	0.3	14.8	9.8	17.0	0.09	135.1	1.6	5.9	n.d.	n.d.	0.97	3.7	5.4	23.8	58.5	0.01	0.00	0.1
Womble	Womble 1	Ordovician	115.1	84.0	105.5	0.9	19.1	25.7	1.4	0.05	598.8	11.3	2.3	0.71	2.0	0.86	0.2	−1.4	1.4	22.5	0.03	0.01	0.0
Womble	Womble 2	Ordovician	73.6	8.1	11.0	0.3	3.1	4.2	1.8	0.03	126.4	1.0	1.6	1.04	1.7	0.96	1.5	1.2	9.1	9.5	0.02	0.00	0.0
Womble	Womble 3	Ordovician	78.1	8.2	10.6	0.3	3.0	4.04	1.8	0.03	127.3	1.1	1.6	0.49	3.7	0.96	1.4	1.2	9.5	9.9	0.02	0.00	0.0
Womble	Womble 3 (D)	Ordovician	267.8	77.6	135.6	2.6	50.4	15.4	0.7	0.2	319.2	7.3	3.0	n.d.	n.d.	0.84	0.4	0.6	3.5	19.7	0.30	0.03	0.0
Mazarn	Mazarn 1	Ordovician	210.8	28.5	94.6	2.1	23.0	28.6	0.8	0.6	84.5	3.3	2.1	0.38	2.0	0.90	0.6	1.0	7.4	11.0	0.83	0.02	0.3
Mazarn	Mazarn 2	Ordovician	96.0	60.6	157.1	2.5	33.6	72.4	0.5	0.8	423.3	5.4	1.6	1.10	0.5	0.74	0.3	−0.2	1.6	13.6	1.50	0.04	0.2
Mazarn	Mazarn 3	Ordovician	9.87	7.4	118.7	1.5	11.7	345.4	0.2	0.02	16.1	0.6	0.3	8.75	0.0	0.46	0.5	0.1	1.3	8.0	0.09	0.02	21.4
Mazarn	Mazarn 4	Ordovician	94.9	54.6	227.8	4.9	19.2	39.2	0.1	0.2	343.5	5.1	1.1	1.31	0.1	0.83	0.2	−0.6	1.7	3.9	1.23	0.11	0.1
Collier	Collier CS1	Camb.-Ordo.	346.0	42.0	77.1	3.6	27.5	54.5	7.2	3.3	278.8	5.4	5.3	2.46	2.9	0.93	1.0	3.5	8.2	7.6	0.46	0.03	0.2
Collier	Collier CS1 (R)	Camb.-Ordo.	349.4	42.5	78.4	3.6	27.8	55.6	7.3	3.4	276.8	5.4	5.3	n.d.	n.d.	0.93	1.0	3.5	8.2	7.6	0.46	0.03	0.2
Tunnel City	UPH-1-658	Cambrian	61.1	92.2	223.2	8.1	28.1	36.6	0.2	0.2	260.5	4.0	0.8	1.61	0.1	0.69	0.2	−0.5	0.7	3.5	1.15	0.18	0.1
Eau Claire	HwyA-2-520	Cambrian	50.3	64.2	233.8	10.3	23.1	47.6	0.3	0.08	131.2	4.3	0.4	1.42	0.2	0.69	0.1	−1.0	0.8	2.2	0.30	0.24	0.4
Eau Claire	UPH-1-853	Cambrian	71.2	79.5	157.8	26.1	48.0	28.2	0.6	0.09	131.4	2.9	0.5	0.73	0.7	0.60	0.2	−0.5	0.9	1.8	0.16	0.41	0.2
Eau Claire	UPH-1-977	Cambrian	80.3	95.5	61.0	8.9	26.9	32.5	0.5	0.1	112.6	1.8	0.4	0.22	2.2	0.75	0.2	−0.2	0.8	3.0	0.24	0.05	0.3
Mt. Simon	UPH-1-1363	Cambrian	79.8	139.3	75.4	8.4	37.1	95.3	0.2	0.2	193.4	3.6	1.0	0.16	1.3	0.68	0.3	−0.2	0.6	4.4	0.96	0.06	0.5

Abbreviations: D = duplicate; ID = identification; HwyA = Highway A; n.d. = no data; R = replicate; *TOC* = total organic carbon.

RESULTS

TOC

The *TOC* results show that many samples have <5% *TOC* (45 samples), 10 samples have 5%–10% *TOC*, and 14 samples have more than 10% *TOC*. All samples >10% *TOC* are Pennsylvanian shales (Table 2). These values are similar to the reported values from other researchers (Figure 3) (James, 1970; Curiale, 1983; Fowler and Douglas, 1984; Ece, 1985; Wenger et al., 1988; Desborough et al., 1990; Schultz and Coveney, 1992; Weber, 1994; Sutton and Land, 1996; Hatch and Leventhal, 1997; Spötl et al., 1998; Bisnett, 2001; Akanbi, 2008; Bamijoko, 2010; Parsell, 2011; Alase, 2012; Liu et al., 2019). The midcontinent Pennsylvanian shales analyzed have *TOC* values between 3.80% and 37.01%, with most being >10%. The samples with the lowest *TOC* are one sample of the Hushpuckney Shale (3.80%) and the Vilas Shale (5.07%). The Atoka and Jackfork Formations have similar *TOC* values (0.91%–1.79% and 0.80%–2.65%, respectively). The Chattanooga and Fayetteville Shales also have similar values (1.91%–7.66% and 0.45%–8.44%, respectively). The Ouachita shales vary in their *TOC* content but are typically <5%. The Cambrian shales from the northern midcontinent have <2% *TOC*.

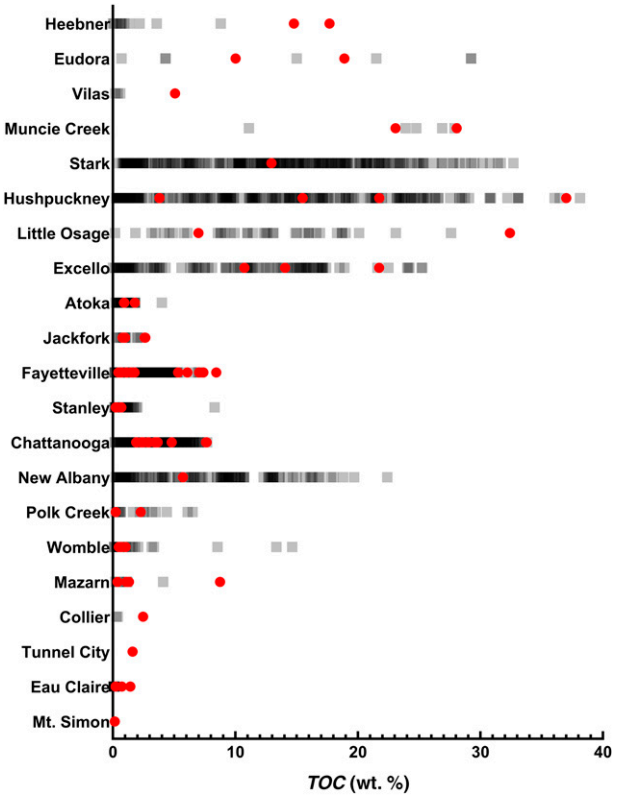

Figure 3. Reported total organic carbon (*TOC*) values of the shales analyzed in this study (red dots) relative to data reported by other researchers (gray squares) illustrating the range of *TOC* in the studied shales (James, 1970; Curiale, 1983; Fowler and Douglas, 1984; Ece, 1985; Wenger et al., 1988; Desborough et al., 1990; Schultz and Coveney, 1992; Weber, 1994; Sutton and Land, 1996; Hatch and Leventhal, 1997; Spötl et al., 1998; Bisnett, 2001; Akanbi, 2008; Bamijoko, 2010; Parsell, 2011; Alase, 2012; Liu et al., 2019). Multiple data points of similar values from other researchers are indicated by darker shades of gray.

Paleoredox Proxies

The bimetal ratios V/(V+Ni), V/Cr, and Ni/Co, as well as U/Th and authigenic U, are not in complete agreement with each other using the thresholds defined by Jones and Manning (1994) (Figure 4). Concentration data for the analyzed elements are presented in Table 2. The V/(V+Ni) model (Figure 4A) defines all but one sample's average value (Stark Shale) within the anoxic or euxinic thresholds, whereas the Stark sample is defined as within the dysoxic field. The U/Th and authigenic U models (Figure 4B and C, respectively) show similar results to each other, with the authigenic U model favoring additional samples within the oxic range. Similarly, the V/Cr and Ni/Co models (Figure 4D and E, respectively) also suggest similar results to each other, although the V/Cr model seems to also favor more samples within the oxic–dysoxic bounds. The ratios in the U/Th, authigenic U, V/Cr, and Ni/Co proxies of the Atoka, Jackfork, and Stanley samples are generally within the oxic thresholds. Poor correlations were found with the Fayetteville, Mazarn, and Vilas samples because these ratios are within both the anoxic and oxic fields. The Chattanooga, New Albany, and Stark Shales have values that generally are within the anoxic and dysoxic limits. The remainder of the samples generally plot within the anoxic fields.

Molybdenum has been linked to increasing anoxic and euxinic conditions, providing a potentially useful indicator of paleoredox conditions (Wilde et al., 2004; Gordon et al., 2009; Scott and Lyons, 2012; Sweere et al., 2016; Algeo and Liu, 2020). The Mo concentrations (Figure 5A; Table 2) show that the Heebner, Hushpuckney, and Muncie Creek Shales are within the euxinic thresholds. The values show that the

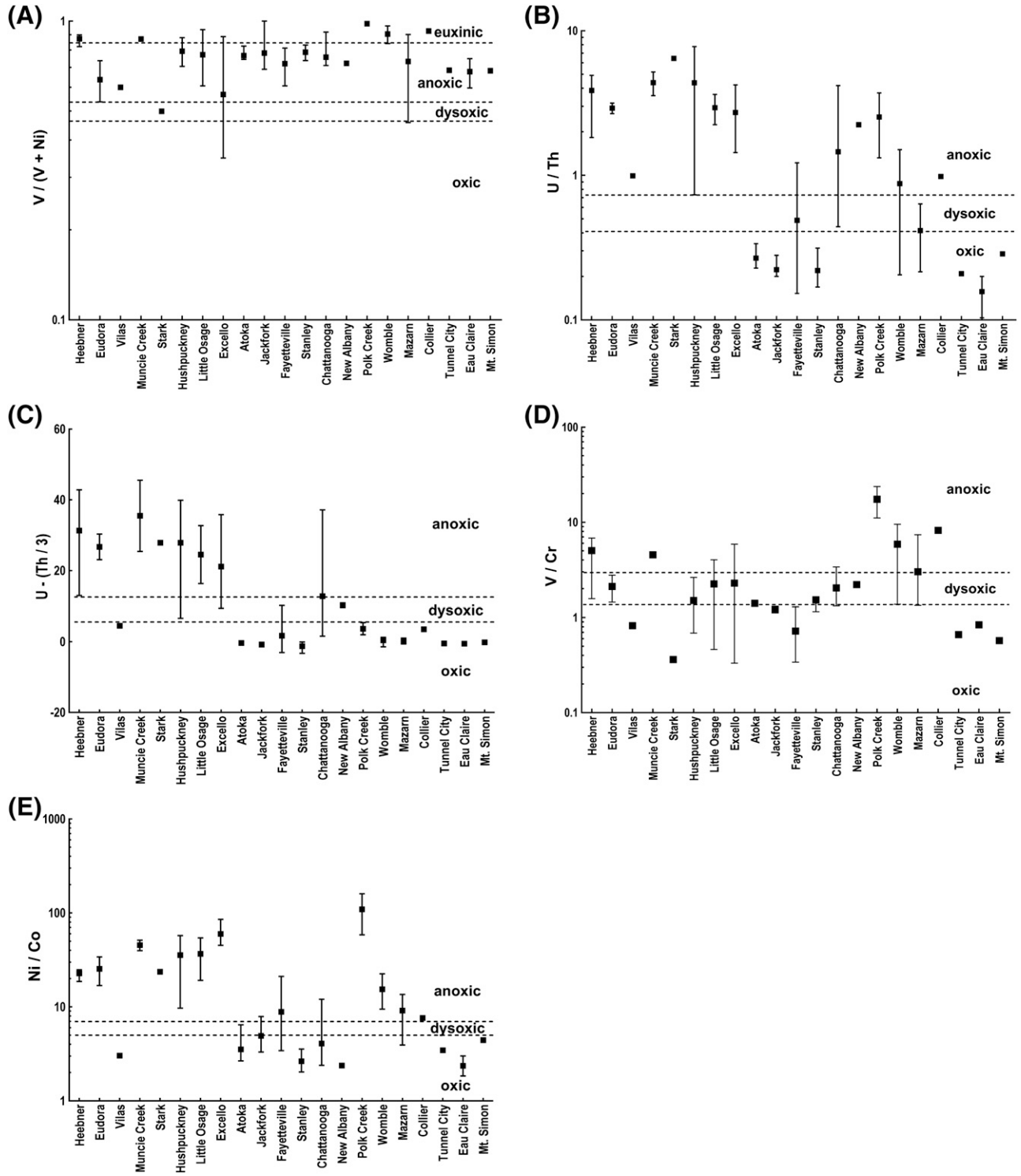

Figure 4. Paleoredox proxies for analyzed samples with the average values (black squares) and the range of values for each shale unit. (A) The V/(V+Ni) proxy has thresholds (dashed horizontal lines) between environments as defined by Hatch and Leventhal (1992). The (B) U/Th proxy, (C) U-(Th/3) proxy, (D) V/Cr proxy, and (E) Ni/Co proxy have thresholds defined by Jones and Manning (1994).

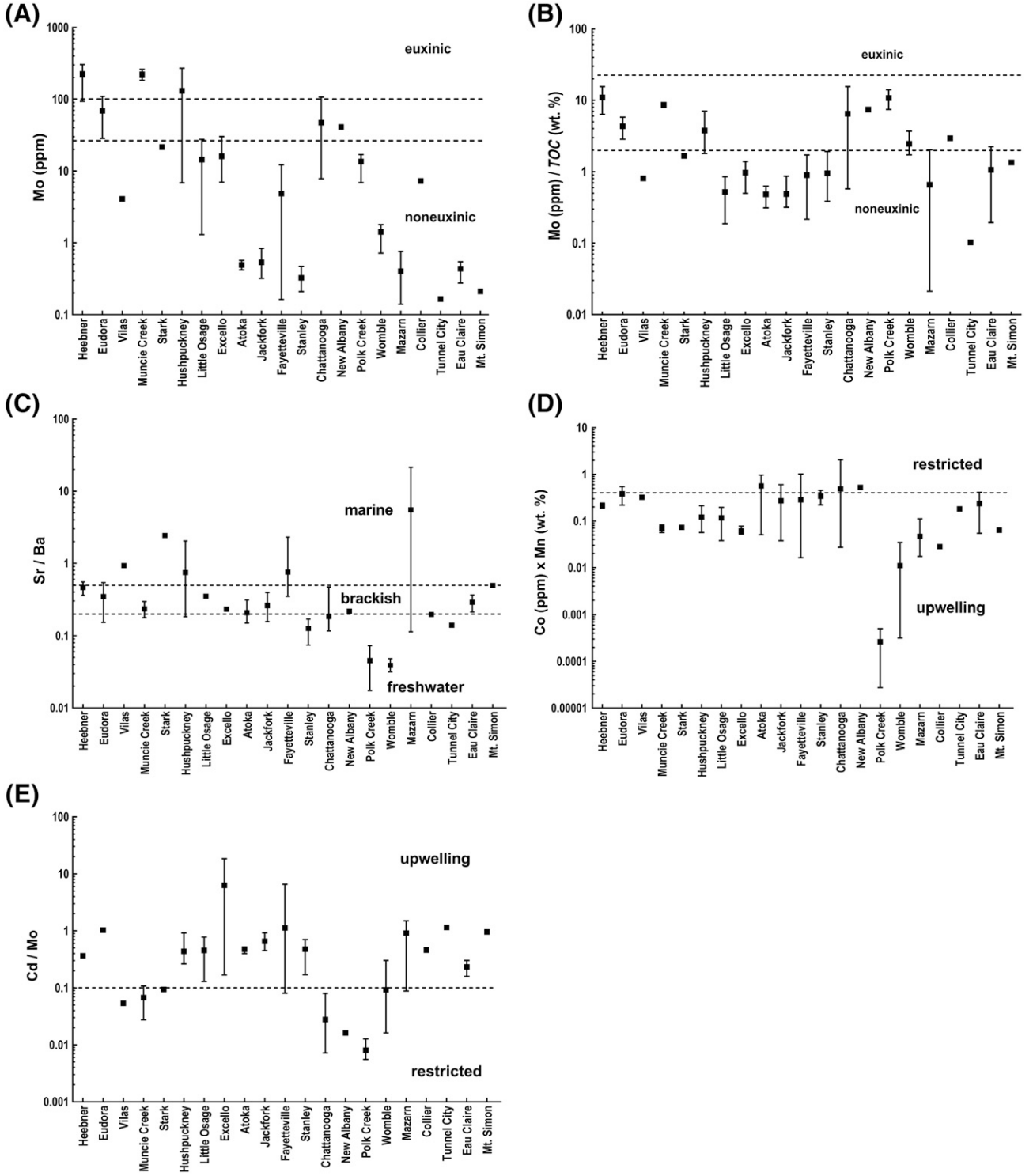

Figure 5. Paleoenvironmental proxies for analyzed samples with the average values (black squares) and the range of values for each shale unit. (A, B) Euxinic/noneuxinic thresholds based on Scott and Lyons (2012) (Mo concentrations, Mo/total organic carbon [*TOC*]). (C) The Sr/Ba average ratios (black squares) with the range of values with thresholds defined by Wei and Algeo (2020). (D, E) Dashed horizontal lines represent thresholds between environments as defined by Sweere et al. (2016).

Heebner (94–305 ppm Mo) and Muncie Creek (184–261 ppm Mo) Shales have concentrations greater than the 100 ppm euxinic threshold of Scott and Lyons (2012), whereas the Hushpuckney Shale has a wider range of Mo concentrations (7–270 ppm) with some samples plotting in the noneuxinic field. The Chattanooga, Eudora, and New Albany Shales have values that span across the boundary between noneuxinic and the intermediate euxinic/noneuxinic fields. The remaining shales generally plot within the noneuxinic bounds according to the Mo concentration model of Scott and Lyons (2012).

When using the Mo (parts per million)/*TOC* (weight percent) ratio proxy (Figure 5B), the highest values were recorded in the Chattanooga (15.6), Heebner (15.5), and Polk Creek (14.1) Shales (Table 2). All other samples have values <10, well under the threshold for euxinic conditions (Mo/*TOC* ≥ 25) of Scott and Lyons (2012). Using the averages for each shale unit, the results show similar trends to those defined by using the Mo (parts per million) concentrations, with a few exceptions. The Heebner, Hushpuckney, and Muncie Creek Shales have averages that plot within the Mo/*TOC* range of the indeterminant sulfide field (2–25) (Scott and Lyons, 2012). The Collier, Womble, and Polk Creek Shales also have averages that plot in the indeterminant sulfide field instead of the noneuxinic conditions as seen in the Mo concentration proxy.

Paleosalinity Proxy

Based on the threshold values of Wei and Algeo (2020), the Sr/Ba paleosalinity proxy indicates that 36 samples are within the freshwater sediment range (<0.2), 30 samples are in the brackish sediment range (0.2–0.5), and 13 samples are in the marine sediment range (>0.5) (Figure 5C; Table 2). The Cambrian and Devonian shale samples from the Illinois Basin are within multiple paleosalinity fields. The Sr/Ba ratios of the Mt. Simon sample are at the brackish–marine boundary (Sr/Ba = 0.493), whereas those of Eau Claire samples (0.215–0.363, average 0.289) are within the range of brackish conditions. The Cambrian Tunnel City sample (0.141) is in the range of the freshwater setting, and the Devonian New Albany Shale samples (0.218–0.221, average 0.220) are along the freshwater–brackish threshold. Similarly, the Sr/Ba ratios of the Pennsylvanian shales from the Cherokee and Forest City Basins are within multiple fields. The Sr/Ba ratios of the Excello (0.221–0.248, average 0.235) and Little Osage (0.340–0.58, average 0.349) Shales fall in the brackish field. The Sr/Ba ratios of the Hushpuckney (0.84–2.046, average 0.746), Stark (2.433), and Vilas (0.932) Shales are in the marine thresholds. The Sr/Ba ratios of the Muncie Creek samples (0.178–0.295, average 0.237) range from freshwater to brackish bounds, whereas those of the Eudora Shale (0.154–0.536, average 0.346) range within freshwater to marine limits. The Heebner Shale samples (0.360–0.552, average 0.462) plot in the brackish to marine domains.

The Sr/Ba ratios of the Devonian Chattanooga Shale (0.117–0.470, average 0.185) in the southwestern Ozark Dome province fall within the freshwater to brackish conditions of Wei and Algeo (2020), whereas those of the Mississippian Fayetteville Shale (0.348–2.308, average 0.756) range within brackish to marine settings. The Sr/Ba ratios of the Ouachita Mountain samples expand across a diverse range of paleosalinity conditions. The Ordovician Womble Shale (0.032–0.048, average 0.039) and Polk Creek Shale (0.017–0.073, average 0.045) and the Mississippian Stanley Shale (0.075–0.171, average 0.127) are limited within the freshwater setting. The Ordovician Mazarn Shale samples (0.114–21.449, average 5.518) range from freshwater to marine settings. The Pennsylvanian Jackfork Sandstone samples (0.173–0.395, average 0.289) range from freshwater to brackish conditions and the Pennsylvanian Atoka Formation samples (0.150–0.311, average 0.210) fall along the freshwater–brackish boundary conditions.

Basin Restriction Proxies

The Co × Mn proxy uses 0.4 as the threshold between upwelling (Co [parts per milllion] × Mn [weight percent] < 0.4) and restricted marine (>0.4) (Sweere et al., 2016). The average Co × Mn values of the Atoka, Chattanooga, and New Albany Shales plot within the confines of restricted marine settings (Figure 5D). All other analyzed shales have average Co × Mn values >0.4, which is within the thresholds of open marine settings with upwelling currents.

The Cd/Mo proxy defines ~0.1 as the threshold between upwelling (>0.1) and restricted marine (<0.1) settings and generally shows similar results to the Co × Mn proxy (Sweere et al., 2016). The Chattanooga,

Muncie Creek, New Albany, Polk Creek, Stark, Vilas, and Womble Shales have Cd/Mo ratios <0.1, falling within restricted marine bounds (Figure 5E; Table 2). Nearly all other samples have minimum values that are greater than 0.1, which firmly places them in the open marine threshold. However, the average Cd/Mo ratios of the Stark and Womble Shale samples are 0.094 and 0.092, respectively, which is along the threshold between the two environmental settings. Sweere et al. (2016) links this proxy to productivity by relating high Cd/Mo ratios (>0.1) with increased organic production (e.g., plankton) driven by upwelling currents, which provide Cd to the sediments upon burial. Low Cd/Mo ratios (<0.1) indicate preservation-driven conditions, with no upwelling currents providing nutrients for organic communities, thus little Cd settles to the sediment (Sweere et al., 2016). When the Cd/Mo ratio is used in conjunction with Co × Mn, many shales plot within the bounds of open marine environments with high organic productivity (Cd/Mo >0.1) with the exception of the Womble, Polk Creek, Chattanooga, New Albany, Atoka, Jackfork, Eudora, Stark, and Vilas Shales (Figure 6) (Sweere et al., 2016). The Chattanooga and New Albany Shales plot within a range associated with restricted to open marine conditions. The Ordovician samples from the Ouachitas have a pattern showing both a decrease in the Cd/Mo ratios and Co × Mn values over time during the deposition of the Collier to Polk Creek Shales. The Collier and Mazarn Shales are both within the open marine, productive environment fields, but during the deposition of the Womble and Polk Creek Shales, they shift to lower production values that are more similar to the modern Black Sea (Sweere et al., 2016).

DISCUSSION

Understanding the paleoenvironmental conditions during the deposition of shales can be challenging due to discrepancies among the paleoredox proxies. However, by considering the range of values for each proxy, the depositional conditions of these shales can be constrained. These models indicate that many of the analyzed shales were likely exposed to anoxic or dysoxic marine conditions during their formation (Figures 4A–E; 5A, B). The summarized average values are provided in Tables 3 and 4.

Cambrian Shales

Focusing on the Cambrian Mt. Simon, Eau Claire, and Tunnel City Formations in the northern Illinois Basin, these clastic units have generally been interpreted as forming in shallow marine environments,

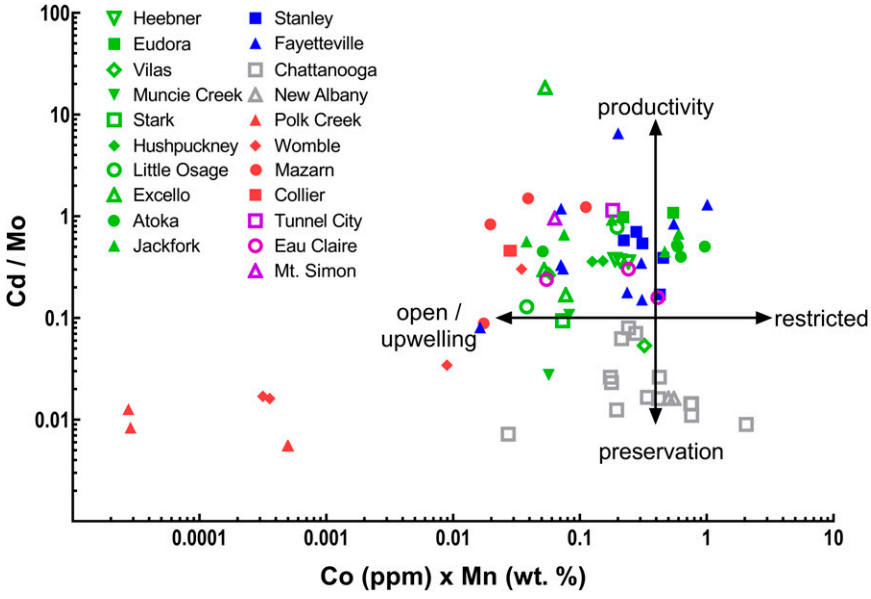

Figure 6. Basin restriction proxy combining the Cd/Mo and Co × Mn proxies. Cambrian samples (purple), Ordovician (red), Devonian (gray), Mississippian (blue), and Pennsylvanian (green); interpretations are based on Sweere et al. (2016).

Table 3. Average Proxy Values with Standard Deviations for Each Shale Formation

Shale Name	V/(V+Ni)		U/Th		Authigenic U		V/Cr		Ni/Co		Mo		Mo/*TOC*		Cd/Mo		Co × Mn		Sr/Ba	
	Avg.	1σ	Avg.	1σ	Avg.	1σ	Avg.	1σ	Avg.	1σ	Avg.	1σ	Avg.	1σ	Avg.	1σ	Avg.	1σ	Avg.	1σ
Atoka	0.766	± 0.033	0.268	± 0.050	−0.372	± 0.293	1.402	± 0.043	3.533	± 1.631	0.493	± 0.072	0.482	± 0.134	0.476	± 0.050	0.563	± 0.328	0.210	± 0.061
Chattanooga	0.758	± 0.052	1.456	± 1.128	12.742	± 11.112	2.039	± 0.508	4.075	± 2.383	29.391	± 31.073	6.486	± 4.810	0.028	± 0.024	0.486	± 0.509	0.185	± 0.097
Collier	0.926	± 0.000	0.982	± 0.004	3.502	± 0.024	8.230	± 0.004	7.625	± 0.004	7.270	± 0.046	2.948	–	0.460	± 0.001	0.028	± 0.001	0.198	± 0.004
Eau Claire	0.677	± 0.076	0.157	± 0.049	−0.567	± 0.381	0.840	± 0.057	2.361	± 0.593	0.436	± 0.142	1.062	± 1.063	0.233	± 0.072	0.236	± 0.178	0.289	± 0.074
Eudora	0.637	± 0.142	2.918	± 0.344	26.699	± 5.110	2.109	± 0.941	25.443	± 12.133	69.152	± 57.425	4.328	± 2.091	1.031	± 0.074	0.381	± 0.229	0.346	± 0.272
Excello	0.568	± 0.283	2.722	± 1.404	21.133	± 13.436	2.286	± 3.105	59.788	± 22.318	16.061	± 12.392	0.971	± 0.448	6.290	± 10.491	0.061	± 0.014	0.235	± 0.014
Fayetteville	0.720	± 0.073	0.488	± 0.373	1.664	± 4.188	0.723	± 0.326	8.857	± 5.932	4.858	± 5.101	0.893	± 0.536	1.129	± 1.955	0.284	± 0.301	0.756	± 0.576
Heebner	0.873	± 0.044	3.868	± 1.768	31.288	± 16.055	5.035	± 3.000	22.753	± 3.568	224.422	± 114.051	10.946	± 6.496	0.365	± 0.010	0.213	± 0.026	0.462	± 0.097
Hushpuckney	0.729	± 0.168	4.366	± 2.832	26.500	± 13.975	1.501	± 1.008	35.570	± 20.697	131.080	± 124.723	3.777	± 2.274	0.437	± 0.273	0.121	± 0.066	0.746	± 0.760
Jackfork	0.743	± 0.050	0.239	± 0.048	−0.713	± 0.494	1.246	± 0.109	4.620	± 1.952	0.535	± 0.222	0.486	± 0.225	0.655	± 0.175	0.272	± 0.249	0.229	± 0.064
Little Osage	0.772	± 0.233	2.936	± 0.981	24.522	± 11.581	2.243	± 2.518	36.675	± 24.812	14.458	± 18.604	0.519	± 0.471	0.454	± 0.460	0.117	± 0.112	0.349	± 0.013
Mazarn	0.733	± 0.195	0.415	± 0.195	0.067	± 0.679	3.013	± 2.925	9.123	± 4.149	0.403	± 0.294	0.657	± 0.930	0.913	± 0.614	0.047	± 0.044	5.518	± 10.621
Mt. Simon	0.682	–	0.286	–	−0.171	–	0.572	–	4.425	–	0.212	–	1.349	–	0.957	–	0.063	–	0.493	–
Muncie Creek	0.872	± 0.006	4.377	± 1.151	35.497	± 14.239	4.545	± 0.019	45.474	± 8.174	222.564	± 54.335	8.642	± 0.933	0.067	± 0.057	0.070	± 0.018	0.237	± 0.083
New Albany	0.722	± 0.001	2.242	± 0.002	10.245	± 0.618	2.205	± 0.002	2.374	± 0.027	41.073	± 1.865	7.408	–	0.016	± 0.000	0.525	± 0.037	0.220	± 0.002
Polk Creek	0.980	± 0.013	2.534	± 1.346	3.654	± 1.929	17.458	± 7.281	109.187	± 58.096	11.007	± 6.989	10.754	± 4.676	0.008	± 0.003	0.0003	± 0.000	0.045	± 0.032
Stanley	0.787	± 0.034	0.220	± 0.057	−1.268	± 1.202	1.520	± 0.211	2.641	± 0.561	0.327	± 0.123	0.952	± 0.671	0.477	± 0.205	0.339	± 0.099	0.127	± 0.038
Stark	0.499	–	6.441	–	27.865	–	0.362	–	23.673	–	21.552	–	1.664	–	0.094	–	0.073	–	2.433	–
Tunnel City	0.685	–	0.209	–	−0.500	–	0.663	–	3.452	–	0.165	–	0.102	–	1.146	–	0.181	–	0.141	–
Vilas	0.600	–	0.993	–	4.481	–	0.823	–	3.033	–	4.088	–	0.806	–	0.054	–	0.322	–	0.932	–
Womble	0.906	± 0.065	0.877	± 0.664	0.381	± 1.254	5.869	± 4.084	15.394	± 6.691	1.422	± 0.506	2.456	± 1.077	0.092	± 0.140	0.011	± 0.016	0.039	± 0.008

Samples with one sample have no standard deviation.
Abbreviations: 1σ = standard deviation; Avg. = Average; *TOC* = total organic carbon.

Table 4. Comparison of Depositional Environments from Various Paleoredox Proxies Based on the Average Values from Samples

Shale Name	Age	V/(V+Ni)	U/Th	Authigenic U	V/Cr	Ni/Co	Mo	Mo/*TOC*	Cd/Mo	Co × Mn	Sr/Ba
Heebner	Pennsylvanian	Euxinic	Anoxic	Anoxic	Anoxic	Anoxic	Euxinic	Uncertain	Upwelling	Upwelling	Brackish
Eudora	Pennsylvanian	Anoxic	Anoxic	Anoxic	Dysoxic	Anoxic	Uncertain	Uncertain	Upwelling	Upwelling	Brackish
Vilas	Pennsylvanian	Anoxic	Anoxic	Oxic	Oxic	Oxic	Noneuxinic	Noneuxinic	Restricted	Upwelling	Marine
Muncie Creek	Pennsylvanian	Euxinic	Anoxic	Anoxic	Anoxic	Anoxic	Euxinic	Uncertain	Restricted	Upwelling	Brackish
Stark	Pennsylvanian	Dysoxic	Anoxic	Anoxic	Oxic	Anoxic	Noneuxinic	Noneuxinic	Restricted	Upwelling	Marine
Hushpuckney	Pennsylvanian	Anoxic	Anoxic	Anoxic	Oxic	Anoxic	Euxinic	Uncertain	Upwelling	Upwelling	Marine
Little Osage	Pennsylvanian	Anoxic	Anoxic	Anoxic	Dysoxic	Anoxic	Noneuxinic	Noneuxinic	Upwelling	Upwelling	Brackish
Excello	Pennsylvanian	Anoxic	Anoxic	Anoxic	Dysoxic	Anoxic	Noneuxinic	Noneuxinic	Upwelling	Upwelling	Brackish
Atoka	Pennsylvanian	Anoxic	Oxic	Oxic	Oxic	Oxic	Noneuxinic	Noneuxinic	Upwelling	Restricted	Brackish
Jackfork	Pennsylvanian	Anoxic	Oxic	Oxic	Oxic	Oxic	Noneuxinic	Noneuxinic	Upwelling	Upwelling	Brackish
Fayetteville	Mississippian	Anoxic	Dysoxic	Oxic	Oxic	Anoxic	Noneuxinic	Noneuxinic	Upwelling	Upwelling	Marine
Stanley	Mississippian	Anoxic	Oxic	Oxic	Oxic	Oxic	Noneuxinic	Noneuxinic	Upwelling	Upwelling	Fresh
Chattanooga	Devonian	Anoxic	Anoxic	Anoxic	Dysoxic	Oxic	Uncertain	Uncertain	Restricted	Restricted	Fresh
New Albany	Devonian	Anoxic	Anoxic	Dysoxic	Dysoxic	Oxic	Uncertain	Uncertain	Upwelling	Restricted	Brackish
Polk Creek	Ordovician	Euxinic	Anoxic	Oxic	Anoxic	Anoxic	Noneuxinic	Uncertain	Restricted	Upwelling	Fresh
Womble	Ordovician	Euxinic	Anoxic	Oxic	Anoxic	Anoxic	Noneuxinic	Uncertain	Restricted	Upwelling	Fresh
Mazarn	Ordovician	Anoxic	Oxic	Oxic	Dysoxic	Anoxic	Noneuxinic	Noneuxinic	Upwelling	Upwelling	Marine
Collier	Cambrian–Ordovician	Euxinic	Anoxic	Oxic	Anoxic	Anoxic	Noneuxinic	Uncertain	Upwelling	Upwelling	Fresh
Eau Claire	Cambrian	Anoxic	Oxic	Oxic	Oxic	Oxic	Noneuxinic	Noneuxinic	Upwelling	Upwelling	Brackish
Tunnel City	Cambrian	Anoxic	Oxic	Oxic	Oxic	Oxic	Noneuxinic	Noneuxinic	Upwelling	Upwelling	Fresh
Mt. Simon	Cambrian	Anoxic	Oxic	Oxic	Oxic	Oxic	Noneuxinic	Noneuxinic	Upwelling	Upwelling	Brackish

Abbreviation: *TOC* = total organic carbon.

spanning from below storm-wave base to intertidal zones (Walcott, 1914; Buschbach, 1975; Driese et al., 1981; Droste and Shaver, 1983; Sargent and Lasemi, 1993; Morse and Leetaru, 2005; Aswasereelert et al., 2008; Eoff, 2014). However, the lower and middle Mt. Simon Formation has been associated with fluvial braided river deposits, with indications of eolian transport (Freiburg et al., 2014).

This study's samples indicate that all three formations—Mt. Simon, Eau Claire, and Tunnel City—were generally deposited under oxic conditions (Figures 4A–E; 5A, B). However, the Tunnel City Formation exhibits a higher Cd/Mo ratio (Figure 5E), suggesting the possibility of deposition under more restricted conditions without significant influence from upwelling currents. The Sr/Ba ratios (Figure 5C) of the Eau Claire and the single sample from the Tunnel City suggest brackish and freshwater settings of Wei and Algeo (2020), respectively. The single sample from the Mt. Simon Shale falls on the threshold between brackish and marine environments. These observations suggest that these shales likely formed under relatively similar conditions that were influenced by freshwater input.

Ordovician Shales

The Ordovician Ouachita shales, including the Collier, Mazarn, Womble, and Polk Creek Shales, are interpreted to have been deposited under generally anoxic and open marine conditions based on the paleoenvironmental proxies. The Lower Ordovician Mazarn Shale indicates a range of oxic to anoxic conditions. The Mo concentration and Mo/*TOC* proxies both suggest that the Mazarn Shale was not deposited in euxinic conditions due to low Mo abundances, indicating a lack of significant H_2S in the environment (Figure 5A, B). Coupled with the V/Cr and Ni/Co ratios, this suggests that persistent euxinia may not have been present, or if it was, it was not widespread, potentially with local or seasonal variations in oxygen and/or sulfide concentrations in the Mazarn Shale.

The Cd/Mo versus Co × Mn proxy (Figure 6) indicates open marine environments among the Mazarn samples with higher organic production than preservation, similar to the Collier Shale. However, the single sample from the Collier Shale suggests deposition under anoxic conditions based on the Ni/Co, V/Cr, U/Th, and V/(V+Ni) proxies (Figure 4A, B, D, E). The presence of disarticulated trilobites suggests that the Collier Shale represents a deposit from the continental slope or deep-water basin, composed of sediment transported from the outer continental shelf (Pitt et al., 1961; Hart et al., 1987; Hohensee and Stitt, 1989; Stitt et al., 1994). However, based on geochemical characteristics of modern continental shelf deposits of Abshire et al. (2020), it is not clear if the Collier was deposited on a distal shelf, but the Mo, V, Ni, and Cu abundances do not preclude the possibility that the overlying Mazarn and Womble Shales were deposited on a shelf slope. Interestingly, the Sr/Ba ratios of the Mazarn Shale (Figure 5C) exhibit the widest range of values among the studied samples, suggesting deposition in freshwater to marine settings. However, only one sample falls within the marine field, suggesting a potential overwhelming influence of fresh water relative to marine waters during the deposition of the Womble Shale, whereas the other samples show similarities to the Collier Shale in terms of Sr/Ba ratios.

The Ordovician Womble Shale appears to have been deposited under anoxic conditions, likely non-euxinic, in open marine settings but with some environmental changes during deposition. The range of Co × Mn values in the analyzed samples indicates the possible influence of upwelling on the depositional environment (Figure 5D). This is supported by the Cd/Mo versus Co × Mn values (Figure 6), which suggest that part of the Womble Shale experienced a productivity-driven environment, but over time, the shales became more preservation-driven (Sweere et al., 2016). Among the studied samples, the Womble Shale shows lower Sr/Ba ratios compared with the Mazarn Shale, possibly indicating a change in sediment source because the Taconic orogeny was contemporaneous with deposition of these Ordovician shales (Gleason et al., 1994, 1995, 2002; Liu, 2020).

The Ordovician Womble and Polk Creek Shales are both inferred to have been deposited under anoxic environments influenced by upwelling (Figures 4A–E; 5A–E). However, they became increasingly preservation-driven, with decreasing Cd/Mo ratios over time compared with the older Cambrian and Ordovician shales (Figure 5E). The Co x Mn values in the Polk Creek Shale fall outside of the range of values used by Sweere et al. (2016) to define modern depositional environments, thus suggesting the possibility of

hydrothermal, diagenetic, or other chemical alterations (Figure 5D; Tables 3, 4). The Sr/Ba ratios present similar conditions as those observed in the Womble Shale (Figure 5C). The increasing relatively high Mo/*T*OC and V/(V+Ni) ratios, and Mo concentrations, suggest a possible transgressive event during the deposition of the Mazarn, Womble, and Polk Creek Shales that led to increasing anoxic and euxinic conditions, as well as increased accumulation of redox-sensitive elements by the end of the Ordovician (Figure 5B).

Devonian Shales

The Devonian Chattanooga Shale of the Ozark Plateaus is interpreted as a widely deposited flooding sequence across much of the midcontinent United States under arid climatic conditions (Lowe, 1975; Parrish, 1982; Kirkland et al., 1992; Houseknecht et al., 2014). Geochemical proxies of this shale suggest deposition in an anoxic or possibly low-oxygen environment (Figures 4A–G; 5A–E). The Cd/Mo versus Co × Mn values indicate that the Chattanooga Shale formed in open to restricted settings, characterized by comparatively low productivity and significant Mo accumulation relative to Cd deposition (Figure 6). The presence of Mo in this and other proxies suggests potential stratification of the water column (Figures 5A, B; 6), possibly leading to anoxic conditions at the sediment–water interface. The Sr/Ba ratios are similar to those reported by Song et al. (2021) and suggest freshwater to brackish settings, which may be attributed to detrital sediment influx into the depositional environment. These proxy results are also comparable with that of the New Albany Shale, suggesting that the Chattanooga and New Albany Shales may have been exposed to similar conditions during their deposition.

Mississippian Shales

Based on trace element concentrations of the Stanley Shale, it has been proposed that this shale was deposited along an active continental margin, involving tectonic collision with mafic (oceanic) crust, possibly through obduction, prior to the deposition of the Stanley Shale (Totten et al., 2000). During this time prior to the Ouachita orogeny, the continents of Laurentia and Gondwana were converging, and it is suggested that a volcanic arc system along the Gondwanan margins served as the source of ash beds in the Stanley Shale (Shaulis et al., 2012). Submarine pyroclastic flows and subsequent settling (and sorting) of ash within the water column have been suggested as the cause of the tuff beds within the Stanley Shale, which have undergone minimal diagenetic alteration (Niem, 1977; Loomis et al., 1994). The Stanley Shale also contains bedded barite deposits (Howard and Hanor, 1987; Hanor, 2000), hypothesized to have formed as a result of tropical/subtropical ocean upwelling, where high productivity occurs at shallow depths and sinking organic matter settles in deeper, low-oxygen environments (Jewell, 1994).

The geochemical proxies (Figures 4A–E; 5A–E) suggest the presence of oxic conditions in a restricted marine setting during the deposition of the Stanley Shale. The Cd/Mo ratios (Figure 5E) indicate that upwelling was unlikely to have occurred in the environment. As paleoproductivity proxies, the Cd/Mo versus Co × Mn values (Figure 6) suggest that the Stanley Shale formed in an environment conducive to productivity but situated near the threshold between open marine and restricted settings. The Sr/Ba ratios (Figure 5C) in this study suggest the presence of fresh water during deposition seemingly in contrast with the deep-water interpretations of Totten et al. (2000) and McFarland (2004). Also, stratabound barite beds have been reported in the Stanley Shale, which have been argued to have developed under anoxic conditions (Zimmerman, 1976; Miller et al., 1977). A possible remedy for this paradox could be sediment gravity flows from the continental shelf to deep-water settings redepositing oxygenated sediments into anoxic deep waters (Hanor and Baria, 1977). Depositional dynamics that formed these barite beds may indicate a limitation of this Sr/Ba proxy (Zimmerman, 1976).

The Late Mississippian Fayetteville Shale is believed to have been formed on a gently dipping continental marine shelf with shallow marine waters ranging from intertidal to depths of up to 200 m (Handford, 1986; Xie et al., 2016). The Cd/Mo and Co × Mn proxies (Figure 5D, E) indicate that the formation of this shale was primarily driven by productivity, with some degree of basin restriction. However, the extent of basin restriction in the Fayetteville Shale remains unclear (Figure 5D, E), whereas the Sr/Ba ratios suggest brackish to marine environments (Figure 5C). The average value of the samples (0.3)

approximates the threshold between open and restricted settings (0.4), indicating an open marine influence. The *TOC* content of the Fayetteville Shale exhibits greater variability compared with the other shales studied, and unlike the other shales, the Fayetteville shows a positive correlation with *TOC* and the enrichment of specific trace elements such as Ni and U. It is uncertain if there is a relationship between *TOC* and the Co × Mn proxy, although no relationship is observed between *TOC* and Cd/Mo.

Pennsylvanian Shales

The Pennsylvanian Jackfork Sandstone is interpreted to have formed in deep-water environments consisting of turbidite deposits from the early stages of the Ouachita orogeny (Morris, 1971; Owen and Carozzi, 1986). The lower to upper Atoka Formation represents a facies change from deep-water deposits to shallow-marine and deltaic deposits (Houseknecht and Ross, 1992; Dickinson et al., 2003). The paleoenvironmental proxy models (Figures 4A–E; 5A–E) suggest that the shales of the Atoka and Jackfork Formations analyzed in this study were deposited in a relatively similar oxic, open marine environment, although the Atoka Formation shows indications of more restricted marine conditions. When interpreted in relation to organic productivity and preservation, the Cd/Mo versus Co × Mn proxy indicates that both the Atoka and Jackfork Formations favored productivity in restricted environments (Figure 6). According to current Sr/Ba ratios (Figure 5C) and previously published results, these formations exhibit similar predominantly brackish waters (Gleason et al., 1995; Reid, 2003; US Geological Survey, 2008; Zou et al., 2017). These ratios may be attributed to the deltaic environment inferred for the Atoka Formation and the submarine slope deposits of the Jackfork Formation (Morris, 1971; Owen and Carozzi, 1986; Houseknecht and Ross, 1992; Dickinson et al., 2003). Considering that these formations consist of thick sequences of clastic sediments that experienced rapid burial and potential hydrothermal alteration during the Ouachita orogeny, hydrothermal influence may also be plausible (Bottoms et al., 2019; Simbo et al., 2019).

The Pennsylvanian black shales analyzed in this study, including the Excello, Little Osage, Hushpuckney, Stark, Muncie Creek, Eudora, and Heebner Shales, exhibit relatively similar paleoredox proxy values. They have some of the highest concentrations of *TOC*, V, Ni, Cr, Mo, Cd, and U among the studied shales (Table 2). The majority of the samples exhibit Sr/Ba ratios indicating brackish to marine settings, with the Stark Shale having the highest Sr/Ba values, suggesting marine conditions (Figure 5C). The proxy models strongly suggest that the Excello, Little Osage, Hushpuckney, and Eudora Shales were deposited under anoxic, noneuxinic conditions (Figures 4A–E; 5A, B). However, the Cd/Mo and Co × Mn proxies (Figure 5D, E) provide conflicting results individually regarding the Cherokee and Forest City Basins' restriction during deposition, except for the Muncie Creek Shale, which indicates open marine conditions in both proxies. When combining the two proxies (Figure 6), most of these Pennsylvanian shales suggest they were formed in productivity-driven open marine environments, except for the Stark, Muncie Creek, and Vilas Shales, which are indicated to have formed under more preservation-driven environments.

The Stark Shale indicates deposition under anoxic conditions, potentially with some dysoxic conditions present (Figures 4A–E; 5A, B). The Cd/Mo ratio and Co × Mn values suggest the possible presence of upwelling (Figure 5D, E), and the Sr/Ba ratios indicate marine settings (Figure 5C). The Heebner Shale appears to have been deposited in strongly anoxic, restricted environments (Figures 4B, C; 5D, E), with the Mo and V/(V + Ni) proxies suggesting the presence of euxinic conditions (Figures 4A, 5A).

The Muncie Creek and Vilas Shales show Cd/Mo ratios and Co × Mn values that suggest the possibility of upwelling (Figure 5D, E), and the Sr/Ba ratios indicate brackish to marine settings (Figure 5C). However, whereas the Vilas Shale exhibits Mo and Mo/*TOC* values indicating noneuxinic depositional settings (Figure 5A, B), the V/(V + Ni) and Mo proxies for the Muncie Creek Shale suggest euxinic conditions (Figures 4A, 5A). The Cd/Mo versus Co × Mn proxy (Figure 6) indicates that the Vilas Shale represents a preservation-driven sequence among the studied Pennsylvanian shales.

Assessing the Reliability of Proxies

This study highlights the importance of using multiple paleoenvironmental proxies to develop an interpretation of the depositional environments of shales,

especially because of the difficulty in establishing reliable geochemical proxies (Jones and Manning, 1994; Averyt and Paytan, 2004; Anderson and Winckler, 2005; Algeo and Liu, 2020). The V/(V+Ni) proxy in this study suggests nearly all studied shales formed under anoxic conditions, whereas the other paleoredox proxies exhibit more variation, including oxic conditions in some shales. The Sr/Ba proxy indicates that nearly all samples formed under the influence of brackish or freshwater conditions, or with input of this water, although previous studies have indicated these shales formed in shallow to deep-water marine environments (Hatch and Leventhal, 1997; Aswasereelert et al., 2008; Zou et al., 2017). The Mississippian Stanley Shale is indicated to have formed under oxic conditions with significant freshwater input, as inferred from the proxies employed in this study. However, the strata-bound barite beds within the shale have been contended to originate syngenetically and/or diagenetically under anoxic conditions, promoting the preservation of organically derived Ba (Zimmerman, 1976; Miller et al., 1977). Hanor and Baria (1977) proposed that these beds formed at the base of the shelf slope from the influence of gravity flows during the initiation of the Ouachita orogeny, which supplied sediment derived from the continental shelf. Although the sediments of the Stanley Shale may have initially originated from oxic waters before redeposition as debris flows, subsequent precipitation of barite beds may have occurred under anoxic, deep-water conditions. Therefore, geochemical indicators suggesting deposition in conditions present on continental shelves, may be retained after sediment redeposition via gravity flows into deep-water settings. Additionally, the relationship between metals and organic matter, such as the Mo/*TOC* proxy, is reliant on the preservation of organic matter to infer depositional conditions because metals can complex with organic matter potentially resulting in higher concentrations of some metals, such as V. However, organic matter sources and compositions have changed throughout the Paleozoic, which may limit the preservational ability of organic matter or the abundance of some metals (Negri et al., 2009).

Differences in these proxies may be attributed to factors that may increase or decrease concentrations of some elements in the depositional or postdepositional environments (e.g., diagenesis, hydrothermal fluids, etc.). Additionally, some proxies have not been well established and may have limitations regarding environmental conditions that could result in inconsistent interpretations, ultimately diminishing their utility (Averyt and Paytan, 2004; Anderson and Winckler, 2005). Therefore, further analysis is needed to assess the reliability of paleoenvironmental proxies with these shales. It is important to note that the number of samples analyzed for these shales is limited, which restricts making comprehensive inferences, but they are valuable for comparative purposes. Additional sampling may also help refine the spatial resolution across the study area and vertically within individual stratigraphic sequences, as well as validate or invalidate the usefulness of these proxies for these shales, especially for those with a limited number of samples.

CONCLUSIONS

A geochemical survey of Paleozoic shales across the midcontinent United States shows that the black shales form under varying depositional conditions, although multiple paleoenvironmental proxies are required to interpret their depositional environment due to the lack of a single, reliable proxy. In the northern Illinois Basin, the Cambrian Mt. Simon, Eau Claire, and Tunnel City Shales are suggested to have formed under oxic, open marine conditions affected by upwelling. The Devonian Chattanooga (Ozark Dome) and New Albany (Illinois Basin) Shales have very similar paleoenvironmental characteristics to each other, indicating they likely formed under dysoxic to anoxic conditions. Unlike the aforementioned rocks, the Mississippian Fayetteville Shale appears to have been exposed to a wider range of conditions, ranging from oxic to anoxic, although it is unclear how these conditions changed over time or spatially during the deposition of the shales. Most proxies imply that the Carboniferous Stanley, Atoka, and Jackfork Formations of the Ouachita Mountains and the Vilas Shale of the Cherokee and Forest City Basins were also deposited under oxic conditions.

The shales with the most strongly anoxic indicators are many of the Cambrian–Ordovician shales of the Ouachita Mountains (Collier, Womble, and Polk Creek) and many of the Pennsylvanian shales of the Cherokee and Forest City Basins (Excello, Little Osage, Hushpuckney, Muncie Creek, Eudora, Heebner).

The paleoredox and basin restriction proxies indicate that the late Cambrian to Early Ordovician Collier Shale formed under anoxic, open marine conditions. This was later followed by the Mazarn Shale, which may have formed under a much wider range of open marine conditions, potentially ranging from oxic to anoxic, but it is unclear what is responsible for this wide range. The overlying Womble and Polk Creek Shales suggest that they both formed under anoxic conditions that may have been influenced by oceanic upwelling currents. However, during the deposition of the Womble Shale, the geochemistry of the environment appears to have changed, becoming increasingly anoxic. This may have been due to a sedimentation rate change during their deposition (Gleason et al., 1994, 1995, 2002; Liu and Algeo, 2020). Many Pennsylvanian black shales of the Cherokee and Forest City Basins (Eudora, Excello, Heebner, Hushpuckney, Little Osage, Muncie Creek, and Stark Shales) that have been described as metalliferous appear to have formed under anoxic and in some cases, euxinic conditions.

REFERENCES CITED

Abshire, M. L., J. D. Owens, J. Cofrancesco, M. Inthorn, and N. Riedinger, 2020, Geochemical signatures of redepositional environments: The Namibian continental margin: Marine Geology, v. 429, 106316, 15 p., doi:10.1016/j.margeo.2020.106316.

Akanbi, O. T., 2008, Paleoclimate and geochemical variation of the Stark Shale Member, Dennis Formation (Missourian), Mid-continent North America, Master's thesis, Texas Tech University, Lubbock, Texas, 129 p.

Alase, A. O., 2012, Gamma spectrometry and geochemical investigation of the Mississippian (Chesterian) Fayetteville Shale and Imo Shale, Arkoma Basin, Arkansas, Master's thesis, Oklahoma State University, Stillwater, Oklahoma, 138 p.

Algeo, T. J., and C. Li, 2020, Redox classification and calibration of redox thresholds in sedimentary systems: Geochimica et Cosmochimica Acta, v. 287, p. 8–26, doi:10.1016/j.gca.2020.01.055.

Algeo, T. J., and J. Liu, 2020, A re-assessment of elemental proxies for paleoredox analysis: Chemical Geology, v. 540, 119549, 12 p., doi:10.1016/j.chemgeo.2020.119549.

Algeo, T. J., and T. W. Lyons, 2006, Mo-total organic carbon covariation in modern anoxic marine environments: Implications for analysis of paleoredox and paleohydrographic conditions: Paleoceanography and Paleoclimatology, v. 21, no. 1, 2004PA001112, 23 p., doi:10.1029/2004PA001112.

Algeo, T. J., and J. B. Maynard, 2004, Trace-element behavior and redox facies in core shales of Upper Pennsylvanian Kansas-type cyclothems: Chemical Geology, v. 206, no. 3–4, p. 289–318, doi:10.1016/j.chemgeo.2003.12.009.

Algeo, T. J., and H. Rowe, 2012, Paleoceanographic applications of trace-metal concentration data: Chemical Geology, v. 324–325, p. 6–18, doi:10.1016/j.chemgeo.2011.09.002.

Algeo, T. J., and N. Tribovillard, 2009, Environmental analysis of paleoceanographic systems based on molybdenum–uranium covariation: Chemical Geology, v. 268, no. 3–4, p. 211–225, doi:10.1016/j.chemgeo.2009.09.001.

Anderson, K. H., and J. S. Wells, 1968, Forest City Basin of Missouri, Kansas, Nebraska, and Iowa: AAPG Bulletin, v. 52, no. 2, p. 264–281.

Anderson, R. F., M. Q. Fleisher, and A. P. LeHuray, 1989, Concentration, oxidation state and particular flux of uranium in the Black Sea: Geochimica et Cosmochimica Acta, v. 53, no. 9, p. 2215–2224, doi:10.1016/0016-7037(89)90345-1.

Anderson, R. F., and G. Winckler, 2005, Problems with paleoproductivity proxies: Paleoceanography, v. 20 no. 3, 2004PA001107, 7 p., doi:10.1029/2004PA001107.

Ardakani, O. H., A. Chappaz, H. Sanei, and B. Mayer, 2016, Effect of thermal maturity on remobilization of molybdenum in black shales: Earth and Planetary Science Letters, v. 449, p. 311–320, doi:10.1016/j.epsl.2016.06.004.

Aswasereelert, W., J. A. Simo, and D. L. LePain, 2008, Deposition of the Cambrian Eau Claire Formation, Wisconsin: Hydrostratigraphic implications of fine-grained cratonic sandstones: Geoscience Wisconsin, v. 19, no. 1, p. 1–21.

Averyt, K. B., and A. Paytan, 2004, A comparison of multiple proxies for export production in the equatorial Pacific: Paleoceanography and Paleoclimatology, v. 19, no. 4, 2004PA001005, 14 p., doi:10.1029/2004PA001005.

Bamijoko, A. O., 2010, Spectrometry and geochemical investigation of selected outcrops of the Chattanooga Shale in the Ozark region of North America, Master's thesis, Oklahoma State University, Stillwater, Oklahoma, 112 p.

Bennett, W. W., and D. E. Canfield, 2020, Redox-sensitive trace metals as paleoredox proxies: A review and analysis of data from modern sediments: Earth-Science Reviews, v. 204, 103175, 11 p., doi:10.1016/j.earscirev.2020.103175.

Bertine, K. K., and K. K. Turekian, 1973, Molybdenum in marine deposits: Geochimica et Cosmochimica Acta, v. 37, no. 6, p. 1415–1434, doi:10.1016/0016-7037(73)90080-X.

Bisnett, A. J., 2001, Petrography and geochemistry of Pennsylvanian black shales in offshore and nearshore stratigraphic settings in Midcontinent and Illinois Basins, Ph.D. dissertation, University of Iowa, Iowa City, Iowa, 469 p.

Boggs, S. Jr., 2006, Principles of sedimentology and stratigraphy: Upper Saddle River, New Jersey, Pearson Prentice Hall, 662 p.

Bottoms, B., A. Potra, J. R. Samuelsen, and S. R. Schutter, 2019, Geochemical investigations of the Woodford-Chattanooga and Fayetteville Shales: Implications for genesis of the Mississippi Valley-type zinc-lead ores in the southern Ozark region and hydrocarbon exploration: AAPG Bulletin, v. 103, no. 7, p. 1745–1768, doi:10.1306/12171818101.

Boucot, A. J., C. Xu, C. R. Scotese, and R. J. Morley, 2013, Phanerozoic paleoclimate: An atlas of lithologic indicators of climate: Tulsa, Oklahoma, SEPM Concepts in Sedimentology and Paleontology 11, 30 p.

Bruland, K. W., 1980, Oceanographic distributions of cadmium, zinc, nickel, and copper in the North Pacific: Earth and Planetary Science Letters, v. 47, no. 2, p. 176–198, doi:10.1016/0012-821X(80)90035-7.

Buchanan, R. C., and J. R. McCauley, 2010, Roadside Kansas: A traveler's guide to its geology and landmarks: Lawrence, Kansas, University Press of Kansas, 376 p.

Burchett, R. R., 1971, Guidebook to the geology along portions of the Lower Platte River Valley and Weeping Water Valley of eastern Nebraska: Lincoln, Nebraska, University of Nebraska Conservation and Survey Division, 38 p.

Buschbach, T. C., 1975, Cambrian System, *in* H. B. Willman, E. Atherton, T. C. Buschbach, C. Collinson, J. C. Frye, M. E. Hopkins, J. A. Lineback, J. A. Simon, eds., Handbook of Illinois stratigraphy, Urbana, Illinois, Illinois State Geological Survey Bulletin 95, p. 34–46.

Calvert, S., and T. Pedersen, 1993, Geochemistry of recent oxic and anoxic marine sediments: Implications for the geological record: Marine Geology, v. 113, no. 1–2, p. 67–88, doi:10.1016/0025-3227(93)90150-T.

Calvert, S. E., and D. Z. Piper, 1984, Geochemistry of ferromanganese nodules from DOMES site a, northern equatorial Pacific: Multiple diagenetic metal sources in the deep sea: Geochimica et Cosmochimica Acta, v. 48, no. 10, p. 1913–1928, doi:10.1016/0016-7037(84)90374-0.

Chinn, A. A. V., and R. H. König, 1973, Stress inferred from calcite twin lamellae in relation to regional structure of northwest Arkansas: GSA Bulletin, v. 84, no. 11, p. 3731–3736, doi:10.1130/0016-7606(1973)84<3731:SIFCTL>2.0.CO;2.

Conway, T. M., and S. G. John, 2015, Biogeochemical cycling of cadmium isotopes along a high-resolution section through the North Atlantic Ocean: Geochimica et Cosmochimica Acta, v. 148, p. 269–283, doi:10.1016/j.gca.2014.09.032.

Coveney, R. M. Jr., 2003, Metalliferous Paleozoic black shales and associated strata, *in* D. R. Lenz ed., Inorganic geochemistry of sediments and sedimentary rocks: Evolutionary considerations to mineral deposit-forming environments: St. John's, Canada, Geological Association of Canada, p. 135–144.

Coveney, R. M. Jr., and M. D. Glascock, 1989, A review of the origins of metal-rich Pennsylvanian black shales central U.S.A., with an inferred role for basinal brines: Applied Geochemistry, v. 4, no. 4, p. 347–367, doi:10.1016/0883-2927(89)90012-7.

Crombez, V., S. Rohais, T. Euzen, L. Riquier, F. Baudin, and E. Hernandez-Bilbao, 2020, Trace metal elements as paleoenvironmental proxies: Why should we account for sedimentation rate variations?: Geology, v. 48, no. 8, p. 839–843, doi:10.1130/G47150.1.

Crusius, J., S. Calvert, T. Pedersen, and D. Sage, 1996, Rhenium and molybdenum enrichments in sediments as indicators of oxic, suboxic and sulfidic conditions of deposition: Earth and Planetary Science Letters, v. 145, no. 1–4, p. 65–78, doi:10.1016/S0012-821X(96)00204-X.

Cubitt, J. M., 1979, The geochemistry, mineralogy and petrology of Upper Paleozoic shales of Kansas: Lawrence, Kansas, Kansas Geological Survey Bulletin 217, 117 p.

Curiale, J. A., 1983, Petroleum occurrences and source rock potential of the Ouachita Mountains southeastern Oklahoma: Norman, Oklahoma, Oklahoma Geological Survey Bulletin 135, 65 p.

Das, A., and S. Krishnaswami, 2006, Barium in Deccan basalt rivers: Its abundance, relative mobility and flux: Aquatic Geochemistry, v. 12, no. 3, p. 221–238, doi:10.1007/s10498-005-5856-4.

Desborough, G. A., J. R. Hatch, and J. S. Leventhal, 1990, Geochemical and mineralogical comparison of the Upper Pennsylvanian Stark Shale Member of the Dennis Limestone, east-central Kansas, with the Middle Pennsylvanian Mecca Quarry Shale Member of the Carbondale Formation in Illinois and of the Linton Formation in Indiana, *in* R. I. Grauch and H. L. O. Huyck, eds., Metalliferous black shales and related ore deposits – Proceedings, 1989 United States Working Group Meeting, November 4, 1989, International Geological Correlation Program Project 254: Washington, DC, US Geological Survey Circular 1058, p. 12–30.

Devera, J. A., and G. H. Fraunfelter, 1988, Middle Devonian paleogeography and tectonic relationships east of the Ozark Dome, southeastern Missouri, southwestern Illinois and parts of southwestern Indiana and western Kentucky, *in* N. J. McMillan, A. F. Embry, and D. J. Glass, eds., Devonian of the world: Second International Symposium on the Devonian System, Calgary, Alberta, Canada, August 17–20, 1987, Canadian Society of Petroleum Geologists Memoir 14, v. 2, p. 179–196.

Dickinson, W. R., P. J. Patchett, C. A. Ferguson, N. H. Suneson, and J. D. Gleason, 2003, Nd isotopes of Atoka Formation (Pennsylvanian) turbidites displaying anomalous east-flowing paleocurrents in the frontal Ouachita belt of Oklahoma: Implications for regional sediment dispersal: Journal of Geology, v. 111, no. 6, p. 733–740, doi:10.1086/378337.

Doe, B. R., J. S. Stuckless, and M. H. Delevaux, 1983, The possible bearing of the granite of the UPH deep drill holes, northern Illinois, on the origin of Mississippi Valley ore deposits: Journal of Geophysical Research, v. 88 no. B9, p. 7335–7345, doi:10.1029/JB088iB09p07335.

Driese, S. G., C. W. Byers, and R. H. Dott, 1981, Tidal deposition in the basal Upper Cambrian Mt. Simon Formation in Wisconsin: Journal of Sedimentary Research, v. 51, no. 2, p. 367–381.

Droste, J. B., and R. H. Shaver, 1983, Atlas of Early and Middle Paleozoic paleogeography of the southern Great Lakes area: Bloomington, Indiana, Indiana Geological Survey Special Report 32, 32 p.

Ece, O. I., 1985, Depositional environment, stratigraphy, petrology, paleogeography, and organic thermal maturation of the Desmoinsian cyclothemic Excello black shale in Oklahoma, Kansas, and Missouri: Ph.D. dissertation, University of Tulsa, Tulsa, Oklahoma, 291 p.

Ece, O. I., 1987, Petrology of the Desmoinesian Excello black shale of the midcontinent region of the United States: Clays and Clay Minerals, v. 35, no. 4, p. 262–270, doi:10.1346/CCMN.1987.0350403.

Emerson, S. R., and S. S. Huested, 1991, Ocean anoxia and the concentrations of molybdenum and vandium in seawater: Marine Chemistry, v. 34, no. 3–4, p. 177–196, doi:10.1016/0304-4203(91)90002-E.

Eoff, J. D., 2014, Sedimentary facies of the upper Cambrian (Furongian; Jiangshanian and Sunwaptan) Tunnel City Group, Upper Mississippi Valley: New insight on the old stormy debate: Sedimentary Geology, v. 302, p. 102–121, doi:10.1016/j.sedgeo.2013.09.008.

Erickson, B. E., and G. R. Helz, 2000, Molybdenum (VI) speciation in sulfidic waters: Stability and lability of thiomolybdates: Geochimica et Cosmochimica Acta, v. 64, no. 7, p. 1149–1158, doi:10.1016/S0016-7037(99)00423-8.

Ervin, C. P., and L. D. McGinnis, 1975, Reelfoot Rift: Reactivated precursor to the Mississippi embayment: GSA Bulletin, v. 86, no. 9, p. 1287–1295, doi:10.1130/0016-7606(1975)86<1287:RRRPTT>2.0.CO;2.

Fowler, M. G., and A. G. Douglas, 1984, Distribution and structure of hydrocarbons in four organic-rich Ordovician rocks: Organic Geochemistry, v. 6, p. 105–114, doi:10.1016/0146-6380(84)90031-7.

François, R., 1988, A study on the regulation of the concentrations of some trace elements (Rb, Sr, Zn, Pb, Cu, V, Cr, Ni, Mn, and Mo) in Saanich Inlet sediments, British Colulmbia, Canada: Marine Geology, v. 83, no. 1–4, p. 285–308, doi:10.1016/0025-3227(88)90063-1.

Freiburg, J. T., D. G. Morse, H. E. Leetaru, R. P. Hoss, and Q. Yan, 2014, A depositional and diagenetic characterization of the Mt. Simon Sandstone at the Illinois Basin–Decatur Project carbon capture and storage site: Champaign, Illinois, Illinois State Geological Survey Circular 583, 53 p.

Gleason, J. D., S. C. Finney, and G. E. Gehrels, 2002, Paleotectonic implications of a Mid- to Late-Ordovician provenance shift, as recorded in sedimentary strata of the Ouachita and southern Appalachian Mountains: The Journal of Geology, v. 110, no. 3, p. 291–304, doi:10.1086/339533.

Gleason, J. D., P. J. Patchett, W. R. Dickinson, and J. Ruiz, 1994, Nd isotopes link Ouachita turbidites to Appalachian sources: Geology, v. 22, no. 4, p. 347–350, doi:10.1130/0091-7613(1994)022<0347:NILOTT>2.3.CO;2.

Gleason, J. D., P. J. Patchett, W. R. Dickinson, and J. Ruiz, 1995, Nd isotopic constraints on sediment sources of the Ouachita-Marathon fold belt: Geological Society of America Bulletin, v. 107, no. 10, p. 1192–1210, doi:10.1130/0016-7606(1995)107<1192:NICOSS>2.3.CO;2.

Godderis, Y., and J. Veizer, 2000, Tectonic control of chemical and isotopic composition of ancient oceans; the impact of continental growth: American Journal of Science, v. 300, no. 5, p. 434–461, doi:10.2475/ajs.300.5.434.

Gordon, G. W., T. W. Lyons, G. L. Arnold, J. Roe, B. B. Sageman, and A. D. Anbar, 2009, When do black shales tell molybdenum isotope tales?: Geology, v. 37, no. 6, p. 535–538, doi:10.1130/G25186A.1.

Handford, C. R., 1986, Facies and bedding sequences in shelf-storm-deposited carbonates: Fayetteville Shale and Pitkin Limestone (Mississippian), Arkansas: Journal of Sedimentary Research, v. 56, no. 1, p. 123–137, doi:10.1306/212F88A0-2B24-11D7-8648000102C1865D.

Hanor, J. S., 2000, Barite-celestine geochemistry and environments of formation: Reviews in Mineralogy and Geochemistry, v. 40, no. 1, 193–275, doi:10.2138/rmg.2000.40.4.

Hanor, J. S., and L. R. Baria, 1977, Controls on the distribution of barite deposits in Arkansas, *in* C. G. Stone, ed., Symposium on the Geology of the Ouachita Mountains, vol. II: Little Rock, Arkansas, Arkansas Geological Survey, 1973, p. 42–49.

Harris, J. W., 1985, Stratigraphy of the Cherokee Group, southeastern Kansas, *in* W. L. Watney, A. W. Walton, and J. Doveton, eds., Core studies in Kansas: Sedimentology and diagenesis of economically important rock strata in Kansas: Lawrence, Kansas, Kansas Geological Survey Subsurface Geology 6, p. 66–73.

Hart, W. D., J. H. Stitt, S. R. Hohensee, and R. L. Ethington, 1987, Geological implications of Late Cambrian trilobites from the Collier Shale, Jessieville area, Arkansas: Geology, v. 15, no. 5, p. 447–450, doi:10.1130/0091-7613(1987)15<447:GIOLCT>2.0.CO;2.

Hastings, D. W., S. R. Emerson, and A. C. Mix, 1996, Vanadium in foraminiferal calcite as a tracer for changes in the areal extent of reducing sediments: Paleoceanography and Paleoclimatology, v. 11, no. 6, p. 665–678, doi:10.1029/96PA01985.

Hatch, J. R., and J. S. Leventhal, 1992, Relationship between inferred redox potential of the depositional environment and geochemistry of the Upper Pennsylvanian (Missourian) Stark Shale Member of the Dennis Limestone, Wabaunsee County, Kansas, U.S.A.: Chemical Geology, v. 99, no. 1–3, p. 65–82, doi:10.1016/0009-2541(92)90031-Y.

Hatch, J. R., and J. S. Leventhal, 1997, Early diagenetic partial oxidation of organic matter and sulfides in the Middle Pennsylvanian (Desmoinesian) Excello Shale Member of the Fort Scott Limestone and equivalents, northern Midcontinent region, USA: Chemical Geology, v. 134, no. 4, p. 215–235, doi:10.1016/S0009-2541(96)00006-X.

Hatcher, R. D. Jr., 2002, Alleghanian (Appalachian) orogeny, a product of zipper tectonics: Rotational transpressive continent-continent collision and closing of ancient oceans along irregular margins, *in* J. R. Martínez Catalán, R. D. Hatcher Jr., R. Arenas, and F. Díaz García, eds., Variscan-Appalachian dynamics: The building of the Late Paleozoic basement: Boulder, Colorado, Geological Society of America Special Paper 364, p. 199–208.

Hohensee, S. R., and J. H. Stitt, 1989, Redeposited *Elvinia* Zone (Upper Cambrian) trilobites from the Collier Shale, Ouachita Mountains, west-central Arkansas: Journal of Paleontology, v. 63, no. 6, p. 857–879, doi:10.1017/S0022336000036544.

Hood, A. V. S., N. J. Planavsky, M. W. Wallace, and X. Wang, 2018, The effects of diagenesis on geochemical paleoredox proxies in sedimentary carbonates: Geochimica et

Cosmochimica Acta, v. 232, p. 265–287, doi:10.1016/j.gca.2018.04.022.

Horner, T. J., S. H. Little, T. M. Conway, J. R. Farmer, J. E. Hertzberg, D. J. Janssen, A. J. M. Lough, et al., 2021, Bioactive trace metals and their isotopes as paleoproductivity proxies: An assessment using GEOTRACES-era data: Global Biogeochemical Cycles, v. 35, no. 11, e2020GB006814, 86 p., doi:10.1029/2020GB006814.

Houseknecht, D. W., and L. M. Ross Jr., 1992, Clay minerals in Atokan deep-water sandstone facies, Arkoma Basin: Origins and influence on diagenesis and reservoir quality, *in* D. W. Houseknecht and E. D. Pittman, eds., Origin, diagenesis, and petrophysics of clay minerals in sandstones: Tulsa, Oklahoma, SEPM Special Publication 47, p. 227–278, doi:10.2110/pec.92.47.0227.

Houseknecht, D. W., W. A. Rouse, S. T. Paxton, J. C. Mars, and B. Fulk, 2014, Upper Devonian–Mississippian stratigraphic framework of the Arkoma Basin and distribution of potential source-rock facies in the Woodford–Chattanooga and Fayetteville–Caney shale-gas systems: AAPG Bulletin, v. 98, no. 9, p. 1739–1759, doi:10.1306/03031413025.

Howard, K. W., and J. S. Hanor, 1987, Compositional zoning in the Fancy Hill stratiform barite deposit, Ouachita Mountains, Arkansas, and evidence for the lack of associated massive sulfides: Economic Geology, v. 82, no. 5, p. 1377–1385, doi:10.2113/gsecongeo.82.5.1377.

Hudson, M. R., 2000, Coordinated strike-slip and normal faulting in the southern Ozark Dome of northern Arkansas: Deformation in a late Paleozoic foreland: Geology, v. 28, no. 6, p. 511–514, doi:10.1130/0091-7613(2000)28<511:CSANFI>2.0.CO;2.

Huerta-Diaz, M. A., and J. W. Morse, 1990, A quantitative method for determination of trace metal concentrations in sedimentary pyrite: Marine Chemistry, v. 29, p. 119–144, doi:10.1016/0304-4203(90)90009-2.

Huerta-Diaz, M. A., and J. W. Morse, 1992, Pyritization of trace metals in anoxic marine sediments: Geochimica et Cosmochimica Acta, v. 56, no. 7, p. 2681–2702, doi:10.1016/0016-7037(92)90353-K.

James, G. W., 1970, Stratigraphic geochemistry of a Pennsylvanian black shale (Excello) in the Midcontinent and Illinois Basin, Ph.D. dissertation, Rice University, Houston, Texas, 92 p.

Jewell, P. W., 1994, Paleoredox conditions and the origin of bedded barites along the Late Devonian North American continental margin: Journal of Geology, v. 102, no. 2, p. 151–164, doi:10.1086/629660.

Jewett, J. M., 1933, Some details of the stratigraphy of the Bronson Group of the Kansas Pennsylvanian: Transactions of the Kansas Academy of Science, v. 36, p. 131–136, doi:10.2307/3625341.

Jones, B., and D. A. C. Manning, 1994, Comparison of geochemical indices used for the interpretation of palaeoredox conditions in ancient mudstones: Chemical Geology, v. 111, no. 1–4, p. 111–129, doi:10.1016/0009-2541(94)90085-X.

Jopling, D. W., and K. Cashion, 1959, Regional gravity of Kansas, *in* W. W. Hambleton, ed., Symposium on Geophysics in Kansas: Lawrence, Kansas, Kansas Geological Survey Bulletin 137, p. 121-133.

Keroher, G. C., and others, 1966, Lexicon of geologic names of the United States for 1936–1960: Washington, DC, US Geological Survey Bulletin 1200, pt. 1, 1448 p.

Kirkland, D. W., R. E. Denison, D. M. Summers, J. R. Gormly, K. S. Johnson, and B. J. Cardott, 1992, Geology and organic geochemistry of the Woodford Shale in the Criner Hills and western Arbuckle Mountains, Oklahoma, *in* K. S. Johnson and B. J. Cardott, eds., Source rocks in the southern midcontinent: Norman, Oklahoma, Oklahoma Geological Survey Circular 93, p. 38–69.

Klein, G. deV., and A. T. Hsui, 1987, Origin of cratonic basins: Geology, v. 15, no. 12, p. 1094–1098, doi:10.1130/0091-7613(1987)15<1094:OOCB>2.0.CO;2.

Klinkhammer, G. P., and M. R. Palmer, 1991, Uranium in the oceans: Where it goes and why: Geochimica et Cosmochimica Acta, v. 55, no. 7, p. 1799–1806, doi:10.1016/0016-7037(91)90024-Y.

Knauer, G. A., J. H. Martin, and R. M. Gordon, 1982, Cobalt in north-east Pacific waters: Nature, v. 297, p. 49–51, doi:10.1038/297049a0.

Kolata, D. R., and W. J. Nelson, 1991a, Tectonic history of the Illinois Basin, *in* M. W. Leighton, D. R. Kolata, D. F. Oltz, and J. J. Eidel, eds., Interior cratonic basins: AAPG Memoir 51, p. 263–286, doi:10.1306/M51530C19.

Kolata, D. R., and W. J. Nelson, 1991b, Basin-forming mechanisms of the Illinois Basin, *in* M. W. Leighton, D. R. Kolata, D. F. Oltz, and J. J. Eidel, eds., Interior cratonic basins: AAPG Memoir 51, p. 287–298, doi:10.1306/M51530C20.

Krabbenhöft, A., A. Eisenhauer, F. Böhm, H. Vollstaedt, J. Fietzke, V. Liebetrau, N. Augustin, et al., 2010, Constraining the marine strontium budget with natural strontium isotope fractionations ($^{87}Sr/^{86}Sr^*$, $\delta^{88}/^{86}Sr$) of carbonates, hydrothermal solutions and river waters: Geochimica et Cosmochimica Acta, v. 74, no. 14, p. 4097–4109, doi:10.1016/j.gca.2010.04.009.

Landing, W. M., and K. W. Bruland, 1980, Manganese in the north Pacific: Earth and Planetary Science Letters, v. 49, no. 1, p. 45–56, doi:10.1016/0012-821X(80)90149-1.

Leighton, M. W., and D. R. Kolata, 1991, Selected interior cratonic basins and their place in the scheme of global tectonics: A synthesis, *in* M. W. Leighton, D. R. Kolata, D. F. Oltz, and J. J. Eidel, eds., Interior cratonic basins: AAPG Memoir 51, p. 729–797, doi:10.1306/M51530C36.

Little, S. H., D. Vance, T. W. Lyons, and J. McManus, 2015, Controls on trace metal authigenic enrichment in reducing sediments: Insights from modern oxygen-deficient settings: American Journal of Science, v. 315, no. 2, p. 77–119, doi:10.2475/02.2015.01.

Liu, J., and T. J. Algeo, 2020, Beyond redox: Control of trace-metal enrichment in anoxic marine facies by watermass chemistry and sedimentation rate: Geochimica et Cosmochimica Acta, v. 287, p. 296–317, doi:10.1016/j.gca.2020.02.037.

Liu, K., M. Ostadhassan, P. C. Hackley, T. Gentzis, J. Zou, Y. Yuan, H. Carvajal-Ortiz, R. Rezaee, and B. Bubach,

2019, Experimental study on the impact of thermal maturity on shale microstructures using hydrous pyrolysis: Energy & Fuels, v. 33, no. 10, p. 9702–9719, doi:10.1021/acs.energyfuels.9b02389.

Loomis, J., B. Weaver, and H. Blatt, 1994, Geochemistry of Mississippian tuffs from the Ouachita Mountains and implications for the tectonics of the Ouachita orogen, Oklahoma and Arkansas: GSA Bulletin, v. 106, no. 9, p. 1158–1171, doi:10.1130/0016-7606(1994)106<1158:GOMTFT>2.3.CO;2.

Lowe, D. R., 1975, Regional controls on silica sedimentation in the Ouachita system: GSA Bulletin, v. 86, no. 8, p. 1123–1127, doi:10.1130/0016-7606(1975)86<1123:RCOSSI>2.0.CO;2.

Lowell, G. R., and G. J. Young, 1999, Interaction between coeval mafic and felsic melts in the St. Francois terrane of Missouri, USA: Precambrian Research, v. 95, no. 1–2, p. 69–88, doi:10.1016/S0301-9268(98)00127-2.

Mansour, A., M. Wagreich, T. Gentzis, S. Ocubalidet, S. S. Tahoun, and A. M. T. Elewa, 2020, Depositional and organic carbon-controlled regimes during the Coniacian-Santonian event: First results from the southern Tethys (Egypt): Marine and Petroleum Geology, v. 115, 104285, 18 p., doi: 10.1016/j.marpetgeo.2020.104285.

McBride, J. H., and W. J. Nelson, 1999, Style and origin of mid-Carboniferous deformation in the Illinois Basin, USA—Ancestral Rockies deformation?: Tectonophysics, v. 305, no. 1–3, p. 249–273, doi:10.1016/S0040-1951(99)00015-3.

McFarland, J. D., 2004, Stratigraphic summary of Arkansas: Little Rock, Arkansas, Arkansas Geological Survey Information Circular 36, 44 p.

Meert, J. G., and W. Stuckey, 2002, Revisiting the paleomagnetism of the 1.476 Ga St. Francois Mountains igneous province, Missouri: Tectonics, v. 21, no. 2, 2000TC001265, 19 p., doi:10.1029/2000TC001265.

Miller, R. E., D. A. Brobst, and P. C. Beck, 1977, The organic geochemistry of black sedimentary barite: Significance and implications of trapped fatty acids: Organic Geochemistry, v. 1, no. 1, p. 11–26, doi:10.1016/0146-6380(77)90005-5.

Moore, R. C., 1932, Kansas, Missouri, Nebraska: Guidebook: Kansas Geological Society Sixth Annual Field Conference, August 23–September 3, 1932, 125 p.

Morford, J. L., and S. Emerson, 1999, The geochemistry of redox sensitive trace metals in sediments: Geochimica et Cosmochimica Acta, v. 63, no. 11–12, p. 1735–1750, doi:10.1016/S0016-7037(99)00126-X.

Morris, J. D., 2014, High resolution correlation of Pennsylvanian marine condensed sections from outcrop to subsurface: Master's thesis, Oklahoma State University, Stillwater, Oklahoma, 199 p.

Morris, R. C., 1971, Stratigraphy and sedimentology of Jackfork Group, Arkansas: AAPG Bulletin, v. 55, no. 3, p. 387–402.

Morse, D. G., and H. E. Leetaru, 2005, Reservoir characterization and three-dimensional models of Mt. Simon gas storage fields in the Illinois Basin: Champaign, Illinois, Illinois State Geological Survey Circular 567, 72 p.

Morse, D. G., and G. W. Luther III, 1999, Chemical influences on trace metal-sulfide interactions in anoxic sediments: Geochimica et Cosmochimica Acta, v. 63, no. 19–20, p. 3373–3378, doi:10.1016/S0016-7037(99)00258-6.

Nakagawa, Y., S. Takano, M. L. Firdaus, K. Norisuye, T. Hirata, D. Vance, and Y. Sohrin, 2012, The molybdenum isotopic composition of the modern ocean: Geochemical Journal, v. 46, no. 2, p. 131–141, doi:10.2343/geochemj.1.0158.

Nance, R. D., G. Gutiérrez-Alonso, J. D. Keppie, U. Linnemann, J. B. Murphy, C. Quesada, R. A. Strachan, and N. H. Woodcock, 2010, Evolution of the Rheic Ocean: Gondwana Research, v. 17, no. 2–3, p. 194–222, doi:10.1016/j.gr.2009.08.001.

Negri, A., A. Ferretti, T. Wagner, and P. A. Meyers, 2009, Phanerozoic organic-carbon-rich marine sediments: Overview and future research challenges: Palaeogeography, Palaeoclimatology, Palaeoecology, v. 273, no. 3–4, p. 218–227, doi:10.1016/j.palaeo.2008.10.002.

Nelson, K. D., and J. Zhang, 1991, A COCORP deep reflection profile across the buried Reelfoot Rift, south-central United States: Tectonophysics, v. 197, no. 2–4, p. 271–293, doi:10.1016/0040-1951(91)90046-U.

Nestell, M. K., B. R. Wardlaw, and J. P. Pope, 2016, A well-preserved conodont fauna from the Pennsylvanian Excello Shale of Iowa, U.S.A.: Micropaleontology, v. 62, no. 2, p. 93–114, doi:10.47894/mpal.62.2.01.

Newell, K. D., 1995, Overview of petroleum geology and production in Kansas, *in* N. L. Anderson and D. E. Hedke, eds., Geophysical atlas of selected oil and gas fields in Kansas: Lawrence, Kansas, Kansas Geological Survey Bulletin 237, p. 2–6.

Niem, A. R., 1977, Mississippian pyroclastic flow and ash-fall deposits in the deep-marine Ouachita flysch basin, Oklahoma and Arkansas: GSA Bulletin, v. 88, no. 1, p. 49–61, doi:10.1130/0016-7606(1977)88<49:MPFAAD>2.0.CO;2.

Owen, M. R., and A. V. Carozzi, 1986, Southern provenance of upper Jackfork Sandstone, southern Ouachita Mountains: cathodoluminescence petrology: GSA Bulletin, v. 97, no. 1, p. 110–115, doi:10.1130/0016-7606(1986)97<110:SPOUJS>2.0.CO;2.

Parrish, J. T., 1982, Upwelling and petroleum source beds, with reference to Paleozoic: AAPG Bulletin, v. 66, no. 6, p. 750–774.

Parrish, S., and R. Van Arsdale, 2004, Faulting along the southeastern margin of the Reelfoot Rift in northwestern Tennessee revealed in deep seismic-reflection profiles: Seismological Research Letters, v. 75, no. 6, p. 784–793, doi:10.1785/gssrl.75.6.784.

Parsell, M. J., 2011, Using cyclothemic black shales to create a proxy calculation for borehole TOC estimates: Master's thesis, Oklahoma State University, Stillwater, Oklahoma, 66 p.

Peng, J., 2021, Sedimentology of the Upper Pennsylvanian organic-rich Cline Shale, Midland Basin: From gravity flows to pelagic suspension fallout: Sedimentology, v. 68, no. 2, p. 805–833, doi:10.1111/sed.12811.

Peng, J., 2022, What besides redox conditions? Impact of sea-level fluctuations on redox-sensitive trace-element enrichment patterns in marine sediments: Science China: Earth Sciences, v. 65, no. 10, p. 1985–2004, doi:10.1007/s11430-021-9959-8.

Pitt, W. D., R. R. Cohoon, H. C. Lee, M. G. Robb, and J. Watson, 1961, Ouachita Mountain core area, Montgomery County, Arkansas: AAPG Bulletin, v. 45, no. 1, p. 72–94.

Reid, D. R., 2003, Major, trace and rare earth element whole rick geochemical analyses of the early to middle Paleozoic strata of the Ouachita orogenic belt, Ph.D. dissertation, University of Houston, Houston, Texas, 1419 p.

Roden, E. E., M. R. Leonardo, and F. G. Ferris, 2002, Immobilization of strontium during iron biomineralization coupled to dissimilatory hydrous ferric oxide reduction: Geochimica et Cosmochimica Acta, v. 66, no. 16, p. 2823–2839, doi:10.1016/S0016-7037(02)00878-5.

Sargent, M. L., 1991, Sauk sequence: Cambrian System through Lower Ordovician Series, *in* M. W. Leighton, D. R. Kolata, D. F. Oltz, and J. J. Eidel, eds., Interior cratonic basins: AAPG Memoir 51, p. 75–85, doi:10.1306/M51530C4.

Sargent, M. L., and Z. Lasemi, 1993, Tidally dominated depositional environment for the Mt. Simon Sandstone in central Illinois (abs.): Geological Society of America Abstracts with Programs, v. 25, no. 3, p. 78.

Schultz, R. B., and R. M. Coveney, 1992, Time-dependent changes for Midcontinent Pennsylvanian black shales, U.S.A.: Chemical Geology, v. 99, no. 1–3, p. 83–100, doi:10.1016/0009-2541(92)90032-Z.

Scott, C., and T. W. Lyons, 2012, Contrasting molybdenum cycling and isotopic properties in euxinic versus non-euxinic sediments and sedimentary rocks: Refining the paleoproxies: Chemical Geology, v. 324–325, p. 19–27, doi:10.1016/j.chemgeo.2012.05.012.

Searight, W. V., 1955, Guidebook to the field trip of the second annual meeting of the Association of Missouri Geologists: Rolla, Missouri, Missouri Geological Survey and Water Resources Report of Investigations 20, 44 p.

Shaulis, B. J., T. J. Lapen, J. F. Casey, and D. R. Reid, 2012, Timing and rates of flysch sedimentation in the Stanley Group, Ouachita Mountains, Oklahoma and Arkansas, U.S.A.: Constraints from U-Pb zircon ages of subaqueous ash-flow tuffs: Journal of Sedimentary Research, v. 82, no. 11, p. 833–840, doi:10.2110/jsr.2012.68.

Simbo, C. W., A. Potra, and J. R. Samuelsen, 2019, A geochemical evaluation of the genetic relationship between Ouachita Mountains Paleozoic rocks and the Mississippi Valley-type mineralization in the southern Ozark Region, USA: Ore Geology Reviews, v. 112, 103029, 18 p., doi:10.1016/j.oregeorev.2019.103029.

Simonds, F. W., 1891, The geology of Washington County, *in* Arkansas Geological Survey annual report, 1887–1892: Little Rock, Arkansas, Geological Survey of Arkansas, v. 4, p. 1–154.

Song, Y., G. J. Gilleaudeau, T. J. Algeo, D. J. Over, T. W. Lyons, A. D. Anbar, and S. Xie, 2021, Biomarker evidence of algal-microbial community changes linked to redox and salinity variation, Upper Devonian Chattanooga Shale (Tennessee, USA): GSA Bulletin, v. 133, no. 1–2, p. 409–424, doi:10.1130/B35543.1.

Spötl, C., D. W. Houseknecht, and R. C. Jaques, 1998, Kerogen maturation and incipient graphitization of hydrocarbon source rocks in the Arkoma Basin, Oklahoma and Arkansas: A combined petrographic and Raman spectrometric study: Organic Geochemistry, v. 28, no. 9–10, p. 535–542, doi:10.1016/S0146-6380(98)00021-7.

Statham, P. J., and J. Burton, 1986, Dissolved manganese in the North Atlantic Ocean, 0-35 N.: Earth and Planetary Science Letters, v. 79, no. 1–2, p. 55–65, doi:10.1016/0012-821X(86)90040-3.

Stitt, J. H., J. D. Rucker, N. D. Boyer, and W. D. Hart, 1994, New *Elvinia* Zone (Upper Cambrian) trilobites from new localities in the Collier Shale, Ouachita Mountains, Arkansas: Journal of Paleontology, v. 68, no. 3, p. 518–523, doi:10.1017/S0022336000025890.

Sutton, S. J., and L. S. Land, 1996, Postdepositional chemical alteration of Ouachita shales: GSA Bulletin, v. 108, no. 8, p. 978–991, doi:10.1130/0016-7606(1996)108<0978:PCAOOS>2.3.CO;2.

Sweere, T., S. van den Boorn, A. J. Dickson, and G. J. Reichart, 2016, Definition of new trace-metal proxies for the controls on organic matter enrichment in marine sediments based on Mn, Co, Mo and Cd concentrations: Chemical Geology, v. 441, p. 235–245, doi:10.1016/j.chemgeo.2016.08.028.

Totten, M. W., M. A. Hanan, and B. L. Weaver, 2000, Beyond whole-rock geochemistry of shales: The importance of assessing mineralogic controls for revealing tectonic discriminants of multiple sediment sources for the Ouachita Mountain flysch deposits: GSA Bulletin, v. 112, no. 7, p. 1012–1022, doi:10.1130/0016-7606(2000)112<1012:BWGOST>2.0.CO;2.

Tribovillard, N., T. J. Algeo, T. Lyons, and A. Riboulleau, 2006, Trace metals as paleoredox and paleoproductivity proxies: An update: Chemical Geology, v. 232, no. 1–2, p. 12–32, doi:10.1016/j.chemgeo.2006.02.012.

Tyson, R. V., and T. H. Pearson, 1991, Modern and ancient continental shelf anoxia: An overview, *in* R. V. Tyson and T. H. Pearson, eds., Modern and ancient continental shelf anoxia: Geological Society, London, Special Publications 1991, v. 58, p. 1–24, doi:10.1144/GSL.SP.1991.058.01.01.

US Geological Survey, 2008, Geochemistry of rock samples from the National Geochemical Database: Reston, Virginia, US Geological Survey, accessed January 30, 2022, https://mrdata.usgs.gov/ngdb/rock/.

Van Arsdale, R., and W. Cupples, 2013, Late Pliocene and Quaternary deformation of the Reelfoot Rift: Geosphere, v. 9, no. 6, p. 1819–1831, doi:10.1130/GES00906.1.

Vetter, L., H. J. Spero, S. M. Eggins, C. Williams, and B. P. Flower, 2017, Oxygen isotope geochemistry of Laurentide icesheet meltwater across Termination I.: Quaternary Science Reviews, v. 178, p. 102–117, doi:10.1016/j.quascirev.2017.10.007.

Vorlicek, T. P., M. D. Kahn, Y. Kasuya, and G. R. Helz, 2004, Capture of molybdenum in pyrite-forming sediments: Role of ligand-induced reduction by polysulfides:

Geochimica et Cosmochimica Acta, v. 68, no. 3, p. 547–556, doi:10.1016/S0016-7037(03)00444-7.

Walcott, C. D., 1914, Dikelocephalus and other genera of the Dikelocephalinæ, *in* Cambrian geology and paleontology: Washington, DC, Smithsonian Miscellaneous Collections, v. 57, no. 13, 345–412.

Weber, J. L., 1994, A geochemical study of crude oils and possible source rocks in the Ouachita tectonic province and nearby areas, southeast Oklahoma: Norman, Oklahoma, Oklahoma Geological Survey Special Publication 94-2, 32 p.

Wehrli, B., and W. Stumm, 1989, Vanadyl in natural waters: Adsorption, and hydrolysis promote oxygenation: Geochimica et Cosmochimica Acta, v. 53, no. 1, p. 69–77, doi:10.1016/0016-7037(89)90273-1.

Wei, W., and T. J. Algeo, 2020, Elemental proxies for paleosalinity analysis of ancient shales and mudrocks: Geochimica et Cosmochimica Acta, v. 287, p. 341–366, doi: 10.1016/j.gca.2019.06.034.

Wenger, L. M., D. R. Baker, H. M. Chung, and T. H. McCulloh, 1988, Environmental control of carbon isotope variations in Pennsylvania black-shale sequences, Midcontinent, U.S.A.: Organic Geochemistry, v. 13, no. 4–6, p. 765–771, doi:10.1016/0146-6380(88)90099-X.

Wilde, P., T. W. Lyons, and M. S. Quinby-Hunt, 2004, Organic carbon proxies in black shales: Molybdenum: Chemical Geology, v. 206, no. 3–4, p. 167–176, doi: 10.1016/j.chemgeo.2003.12.005.

Xie, X., W. Cains, and W. L. Manger, 2016, U-Pb detrital zircon evidence of transcontinental sediment dispersal: Provenance of Late Mississippian Wedington Sandstone member, NW Arkansas: International Geology Review, v. 58, no. 15, p. 1951–1966, doi:10.1080/00206814.2016.1193775.

Zimmerman, R. A., 1976, Rhythmicity of barite-shale and of Sr in strata-bound deposits of Arkansas, *in* K. H. Wolf ed., Handbook of strata-bound and stratiform ore deposits, vol. 3, New York, Elsevier Science, p. 339–353.

Zou, F., R. M. Slatt, J. Zhang, and T. Huang, 2017, An integrated chemo- and sequence-stratigraphic framework of the Early Pennsylvanian deepwater outcrops near Kirby, Arkansas, USA, and its implications on remnant basin tectonics: Marine and Petroleum Geology, v. 81, p. 252–277, doi:10.1016/j.marpetgeo.2017.01.006.